

Free Access XPS Instrumentation Funded by EPSRC Grants for UK Academic Use

[University of Nottingham](#)

[University of Cardiff](#)

XPS Spectra

The XPS technique is used to investigate the chemistry at the surface of a sample.

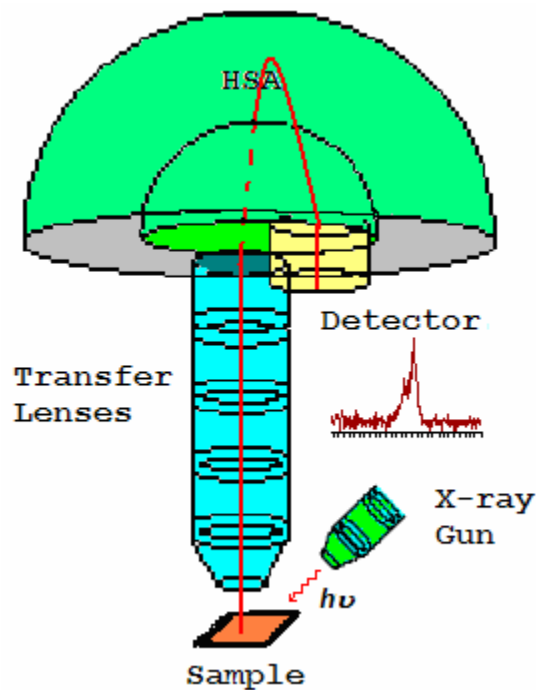


Figure 1: Schematic of an XPS instrument.

The basic mechanism behind an XPS instrument is illustrated in Figure 1, where photons of a specific energy are used to excite the electronic states of atoms below the surface of the sample. Electrons ejected from the surface are energy filtered via a hemispherical analyser (HSA) before the intensity for a defined energy is recorded by a detector. Since core level electrons in solid-state atoms are quantized, the resulting energy spectra exhibit resonance peaks characteristic of the electronic structure for atoms at the sample surface. While the x-rays may penetrate deep into the sample, the escape depth of the ejected electrons is limited. That is, for energies around 1400 eV, ejected electrons from depths greater than 10nm have a low probability of leaving the surface without undergoing an energy loss event, and therefore contribute to the background signal rather than well defined primary photoelectric peaks.

In principle, the energies of the photoelectric lines are well defined in terms of the binding energy of the electronic states of atoms. Further, the chemical environment of the atoms at the surface result in well defined energy shifts to the peak energies. In the case of conducting samples, for which the detected electron energies can be referenced to the Fermi energy of the spectrometer, an absolute energy scale can be established, thus aiding the identification of species. However, for non-conducting samples the problem of energy calibration is significant. Electrons leaving the sample surface cause a potential difference to exist between the sample and the spectrometer resulting in a retarding field acting on the electrons escaping the surface. Without redress, the consequence can be peaks shifted in energy by as much as 150 eV. Charge compensation designed to replace the electrons

emitted from the sample is used to reduce the influence of sample charging on insulating materials, but nevertheless identification of chemical state based on peak positions requires careful analysis.

XPS is a quantitative technique in the sense that the number of electrons recorded for a given transition is proportional to the number of atoms at the surface. In practice, however, to produce accurate atomic concentrations from XPS spectra is not straight forward. The precision of the intensities measured using XPS is not in doubt; that is intensities measured from similar samples are repeatable to good precision. What are doubtful are results reporting to be atomic concentrations for the elements at the surface. An accuracy of 10% is typically quoted for routinely performed XPS atomic concentrations. For specific carefully performed and characterised measurements better accuracy is possible, but for quantification based on standard relative sensitivity factors, precision is achieved not accuracy. Since many problems involve monitoring changes in samples, the precision of XPS makes the technique very powerful.

The first issue involved with quantifying XPS spectra is identifying those electrons belonging to a given transition. The standard approach is to define an approximation to the background signal. The background in XPS is non-trivial in nature and results from all those electrons with initial energy greater than the energy in questions for which scattering events cause energy losses prior to emission from the sample. The zero-loss electrons constituting the photoelectric peak are considered to be the signal above the background

approximation. A variety of background algorithms are used to measure the peak area; none of the practical algorithms are correct and therefore represent a source for uncertainty when computing the peak area. Peak areas computed from the background subtracted data form the basis for most elemental quantification results from XPS.

The data in Figure 2 illustrates an XPS spectrum measured from a typical sample encountered in practice. The inset tile within Figure 2 shows the range of energies associated with the C 1s and K 2p photoelectric lines. Since these two transitions include multiple overlapping peaks, there is a need to apportion the electrons to the C 1s or the K 2p transitions using a synthetic peak model fitted to the data. The degree of correlation between the peaks in the model influences the precision and therefore the accuracy of the peak area computation.

Relative sensitivity factors of photoelectric peaks are often tabulated and used routinely to scale the measured intensities as part of the atomic concentration calculation. These RSF tables can only be accurate for homogenous materials. If the sample varies in composition with depth, then the kinetic energy of the photoelectric line alters the depth from which electrons are sampled. It is not uncommon to see evidence of an element in the sample by considering a transition at high kinetic energy, but find little evidence for the presence of the same element when a lower kinetic energy transition is considered. Transitions of this nature might be Fe 2p compared to Fe 3p both visible in Figure 2, where the relative intensity of these peaks will depend on the depth of the iron with respect to

the surface. Sample roughness and angle of the sample to the analyser also changes the relative intensity of in-homogenous

samples, thus sample preparation and mounting can influence quantification values.

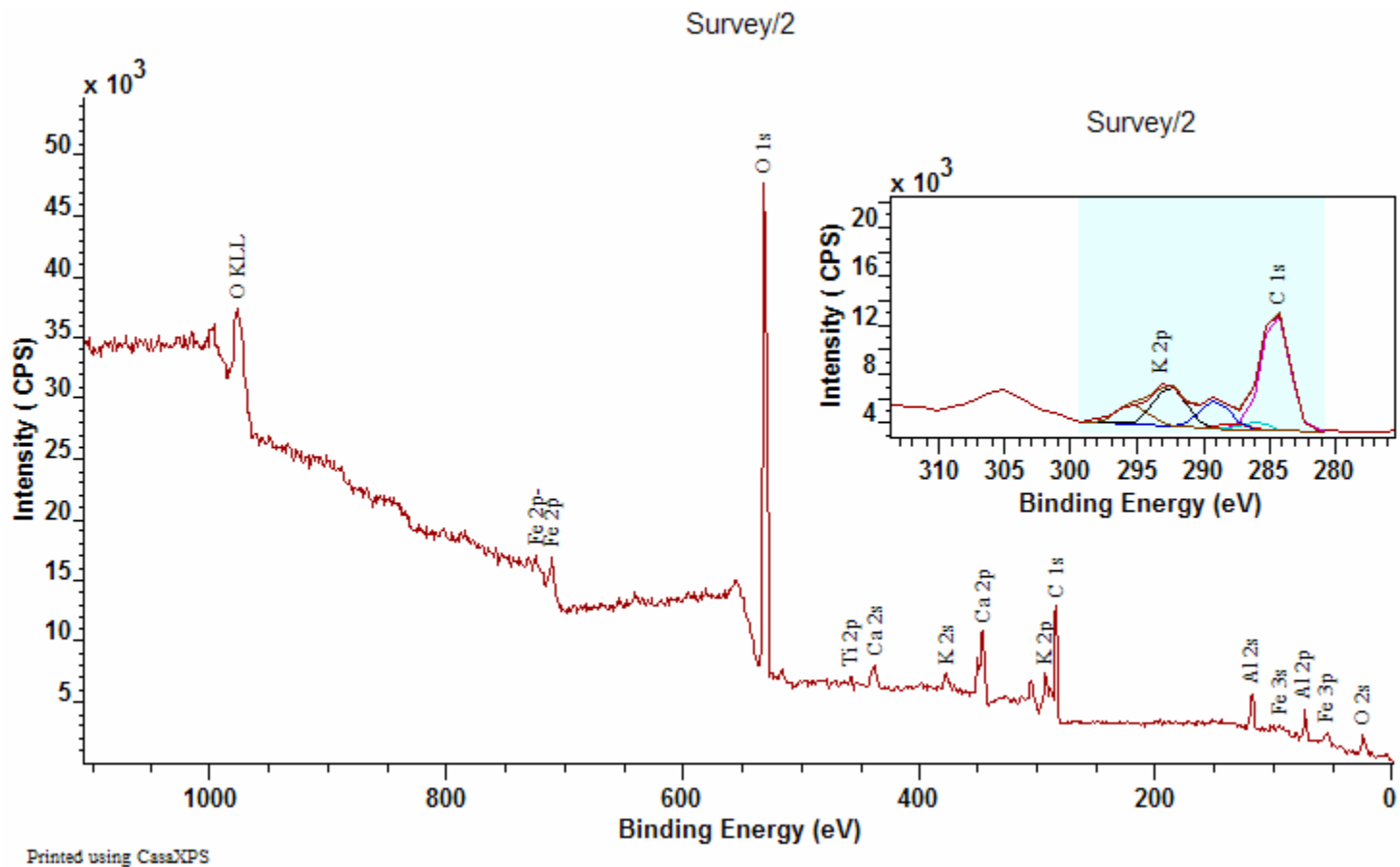
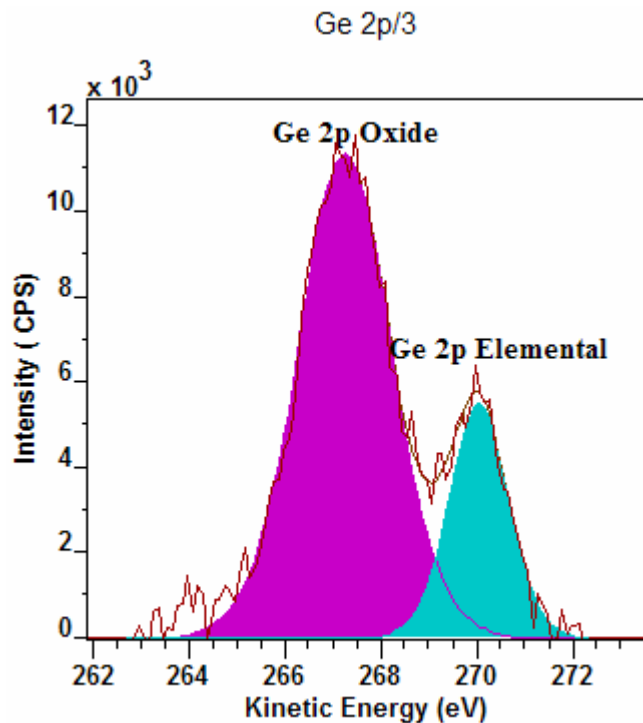


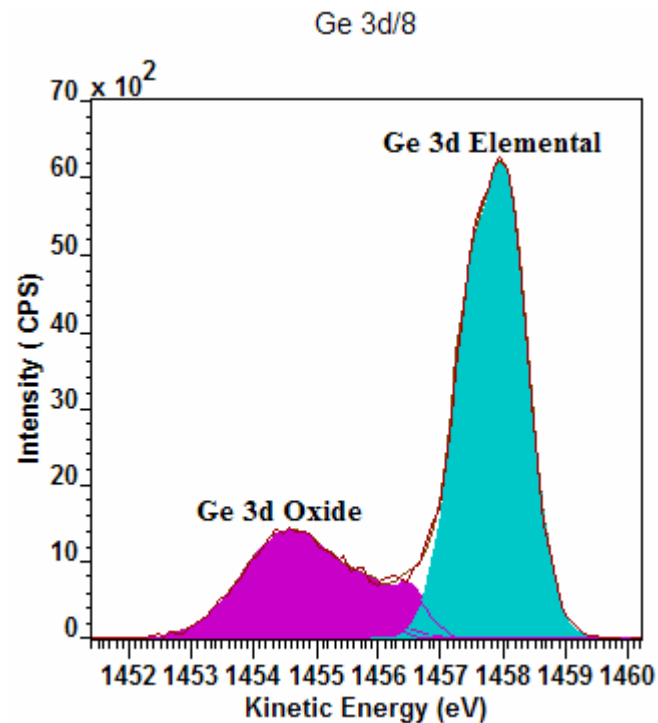
Figure 2: An example of a typical XPS survey spectrum taken from a compound sample.



Printed using CasaXPS

Figure 3: Germanium Oxide relative intensity to elemental germanium measured using photoelectrons with kinetic energy in the range 262 eV to 272 eV.

The chemical shifts seen in XPS data are a valuable source of information about the sample. The spectra in Figure 3 and Figure 4 illustrate the separation of elemental and oxide peaks of germanium due to chemical state. Both spectra were acquired from the same sample under the same conditions with the exception that the ejected electrons for the Ge 3d peaks are about 1200 eV more energetic than the Ge 2p electrons. The



Printed using CasaXPS

Figure 4: Germanium Oxide relative intensity to elemental germanium measured using photoelectrons with kinetic energy in the range 1452 eV to 1460 eV.

consequence of choosing to quantify based on one of these transitions is that the proportion of oxide to elemental germanium differs significantly. The oxide represents an over layer covering of the elemental germanium and therefore the low energy photoelectrons from the Ge 2p line are attenuated resulting in a shallower sampling depth compared to the more energetic Ge 3d electrons. Hence the volume sampled by the

Ge 2p transition favours the oxide signal, while the greater depth from which Ge 3d electrons can emerge without energy loss favours the elemental germanium. While these variations may seem a problem, such changes in the spectra are also a source for information about the sample.

Tilting the sample with respect to the axis of the analyser results in changing the sampling depth for a given transition and therefore data collected at different angles vary due to the differing composition with depth. Figure 5 is a sequence of Si 2p spectra measured from the same silicon sample at different angles. The angles associated with the spectra are with respect to the axis of the analyser and the sample surface. Data measured at 30° favours the top most oxide layers; while at 90° the elemental substrate becomes dominant in the spectrum.

Other Peaks in XPS Spectra

Not all peaks in XPS data are due to the ejection of an electron by a direct interaction with the incident photon. The most notable are the Auger peaks, which are explained in terms of the decay of a more energetic electron to fill the vacant hole created by the x-ray photon, combined with the emission of an electron with an energy characteristic of the difference between the states involved in the process. The spectrum in Figure 1 includes a sequence of peaks labelled O KLL. These peaks represent the energy of the electrons ejected from the atoms due to the filling of the O 1s state (K shell) by an electron from the L shell coupled with the ejection of an electron from an L shell.

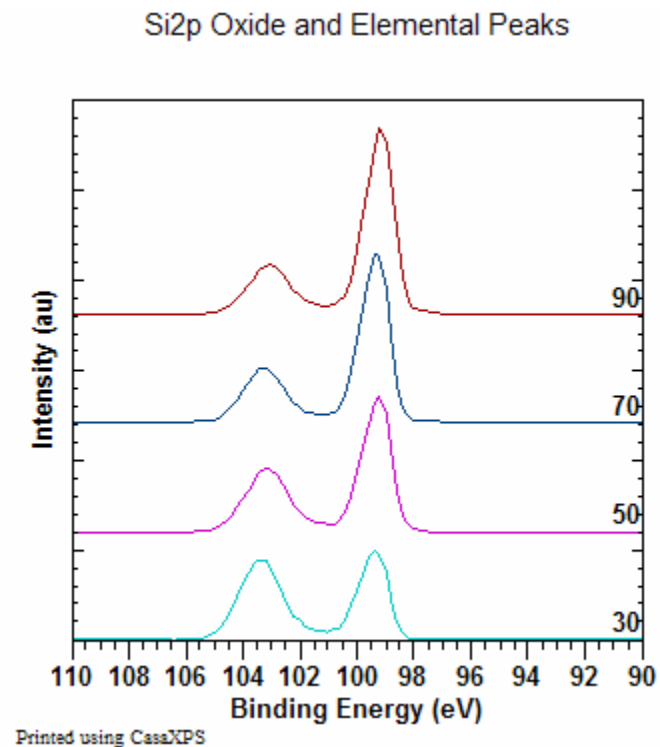


Figure 5: Angle resolved Si 2p spectra showing the changes to the spectra resulting from tilting the sample with respect to the analyser axis.

Unlike the photoelectric peaks, the kinetic energy of the Auger lines is independent of the photon energy for the x-ray source. Since the kinetic energy of the photoelectrons are given in terms of: the photon energy $h\nu$, the binding energy for the ejected electron E_{be} and a work function ϕ by the

relationship $E_{ke} = h\nu - E_{be} - \phi$, altering the photon energy by changing the x-ray anode material causes the Auger lines and the photoelectric lines to move in energy relative to one another.

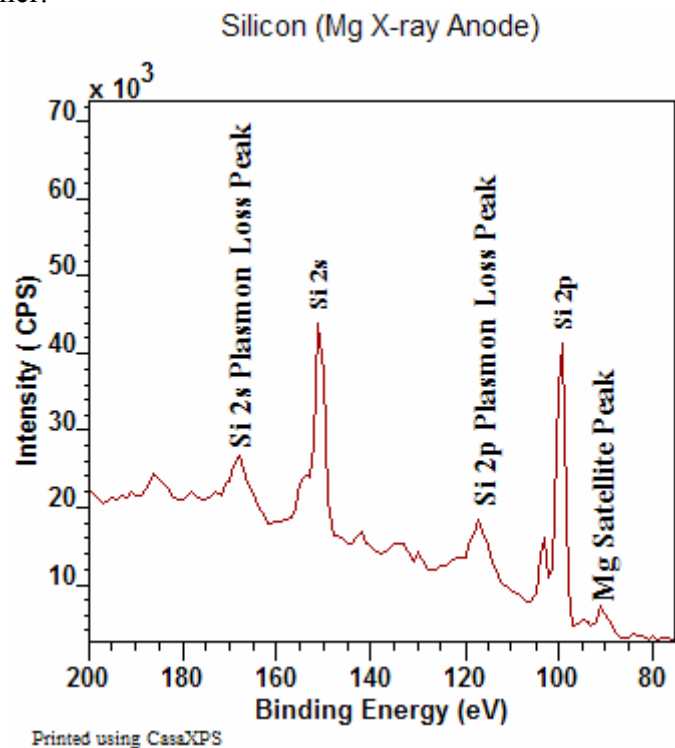


Figure 6: Elemental Silicon loss peaks and also x-ray satellite peak.

Less prominent than Auger lines are x-ray satellite peaks. Data acquired using a non-monochromatic x-ray source create satellite peaks offset from the primary spectral lines by the difference in energy between the resonances in the x-ray

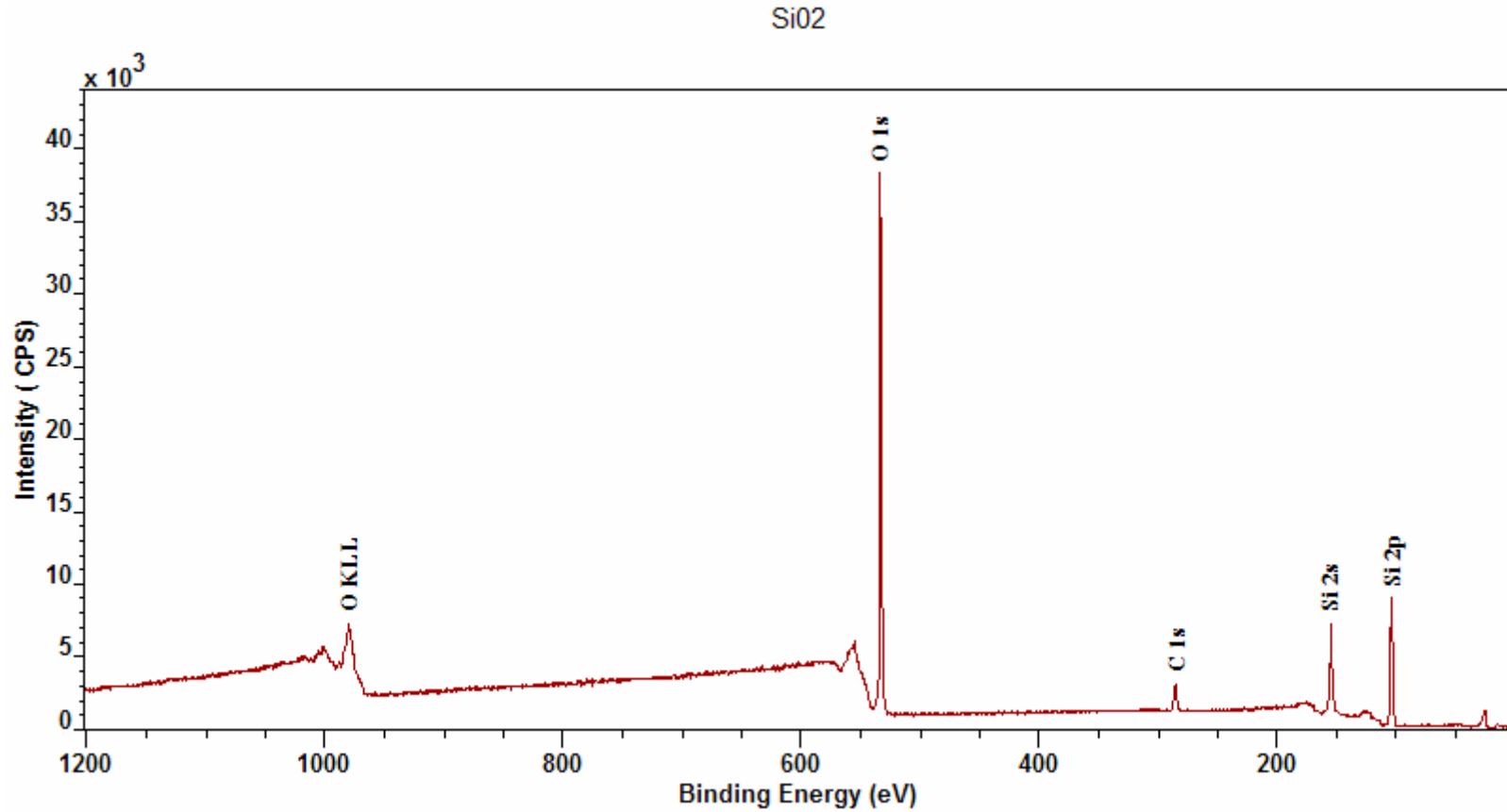
spectrum of the anode material used in the x-ray gun and also in proportion to the peaks in the x-ray spectrum for the anode material. Figure 6 indicates an example of a satellite peak to the primary Si 2p peak due to the use of a magnesium anode in the x-ray source. Note that Auger line energies are independent of the photon energy and therefore do not have satellite peaks.

A further source for peaks in the background signal is due to resonant scattering of electrons by the surface materials. Plasmon peaks for elemental silicon are also labeled on Figure 6. The sharpness of these plasmon peaks in Figure 6 is due to the nature of the material through which the photoelectrons must pass. For silicon dioxide, the loss structures are much broader and follow the trend of a typical XPS background signal. The sharp loss structures in Figure 6 are characteristic of pure metallic-like materials.

The following section is a collection of XPS spectra acquired from a variety of materials. The features touched upon in this introduction to the XPS technique can be seen in these data. No details about these samples are given and the energy calibration is merely nominal in nature; the primary object is to provide an impression of XPS data rather than define reference spectra for comparative purposes.

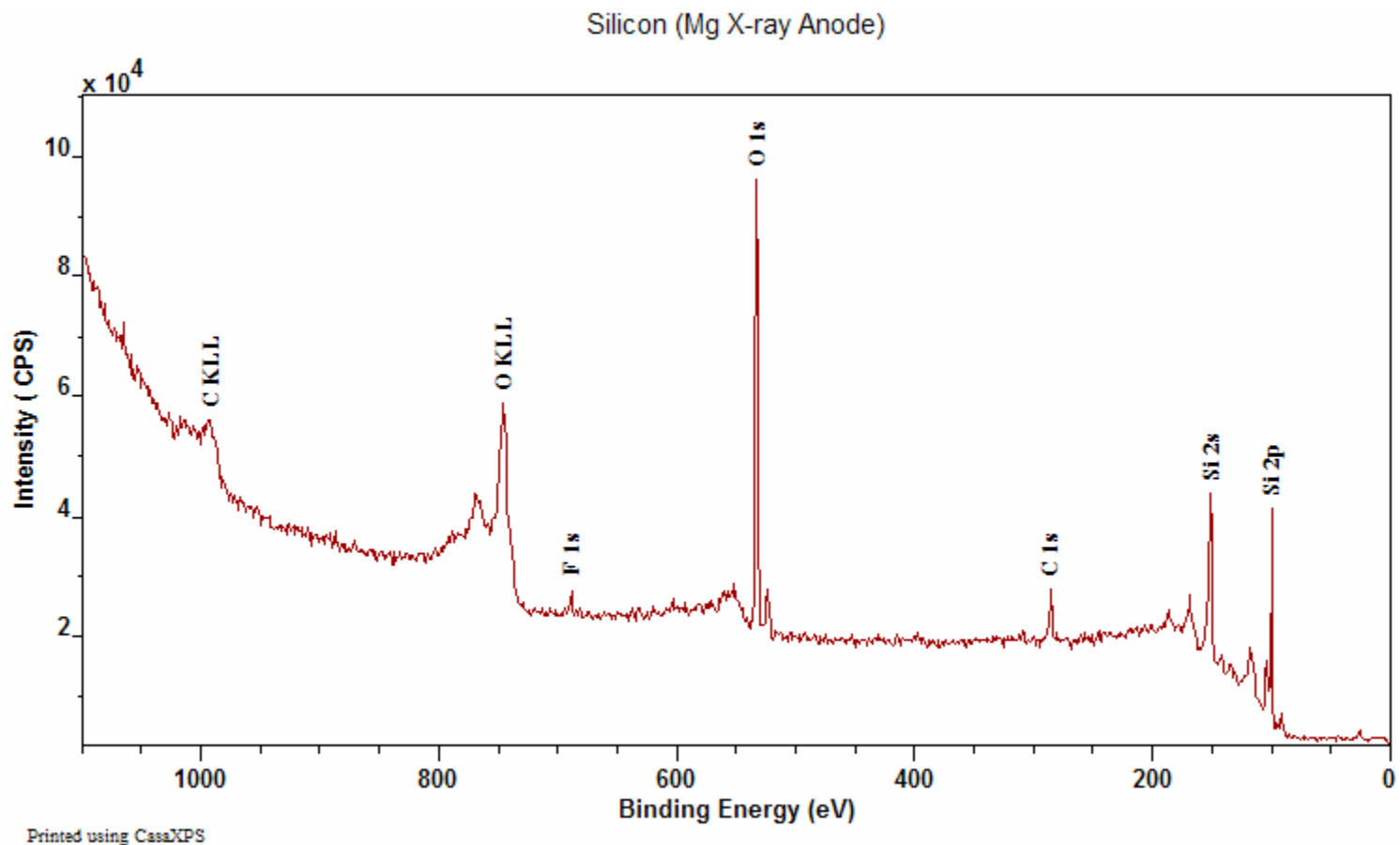
Examples of XPS Spectra

The following spectra are intended to provide examples of XPS survey data illustrating the various structures discussed above.

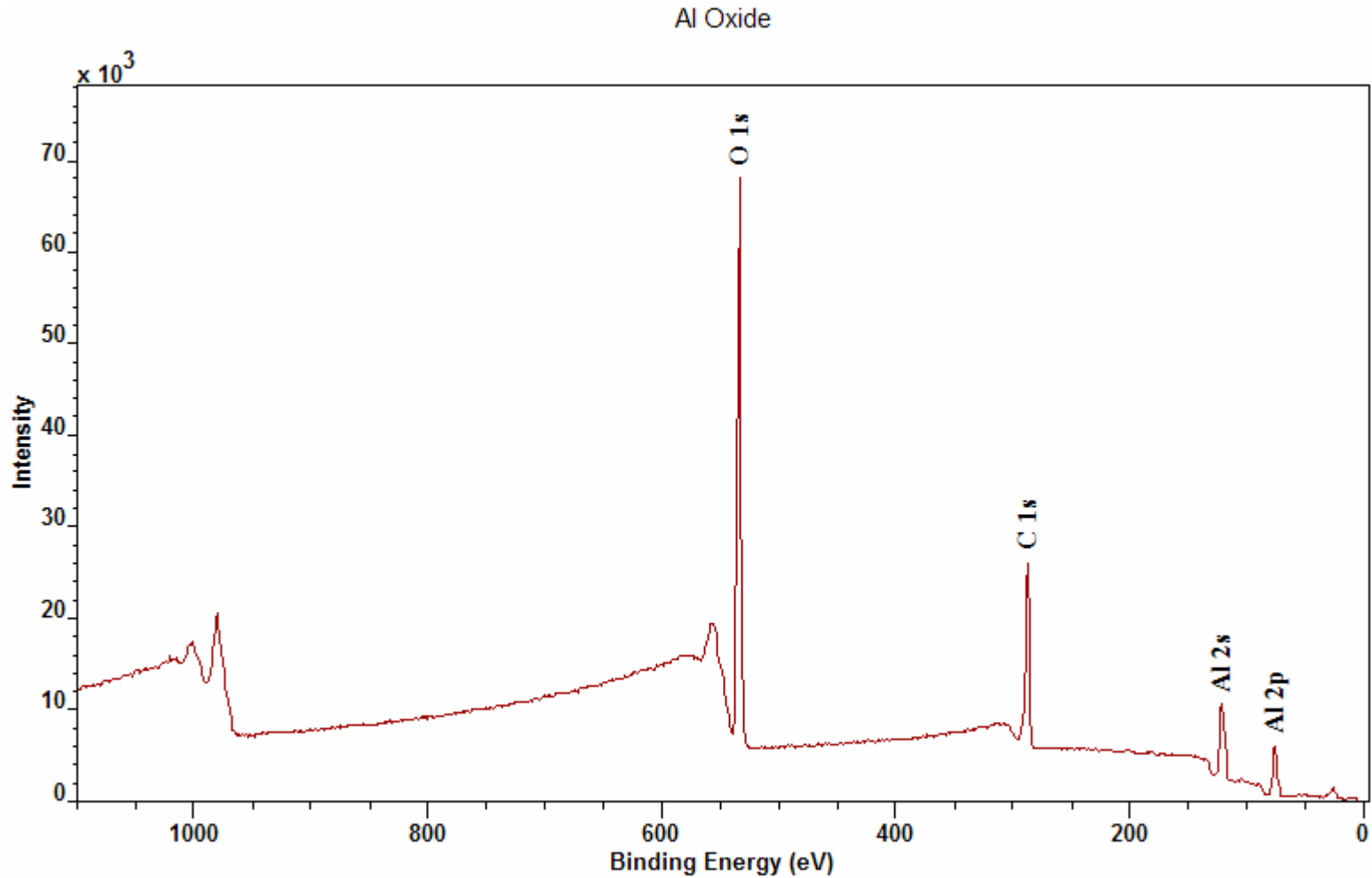


Printed using CasaXPS

SiO₂ measured using an aluminium anode.

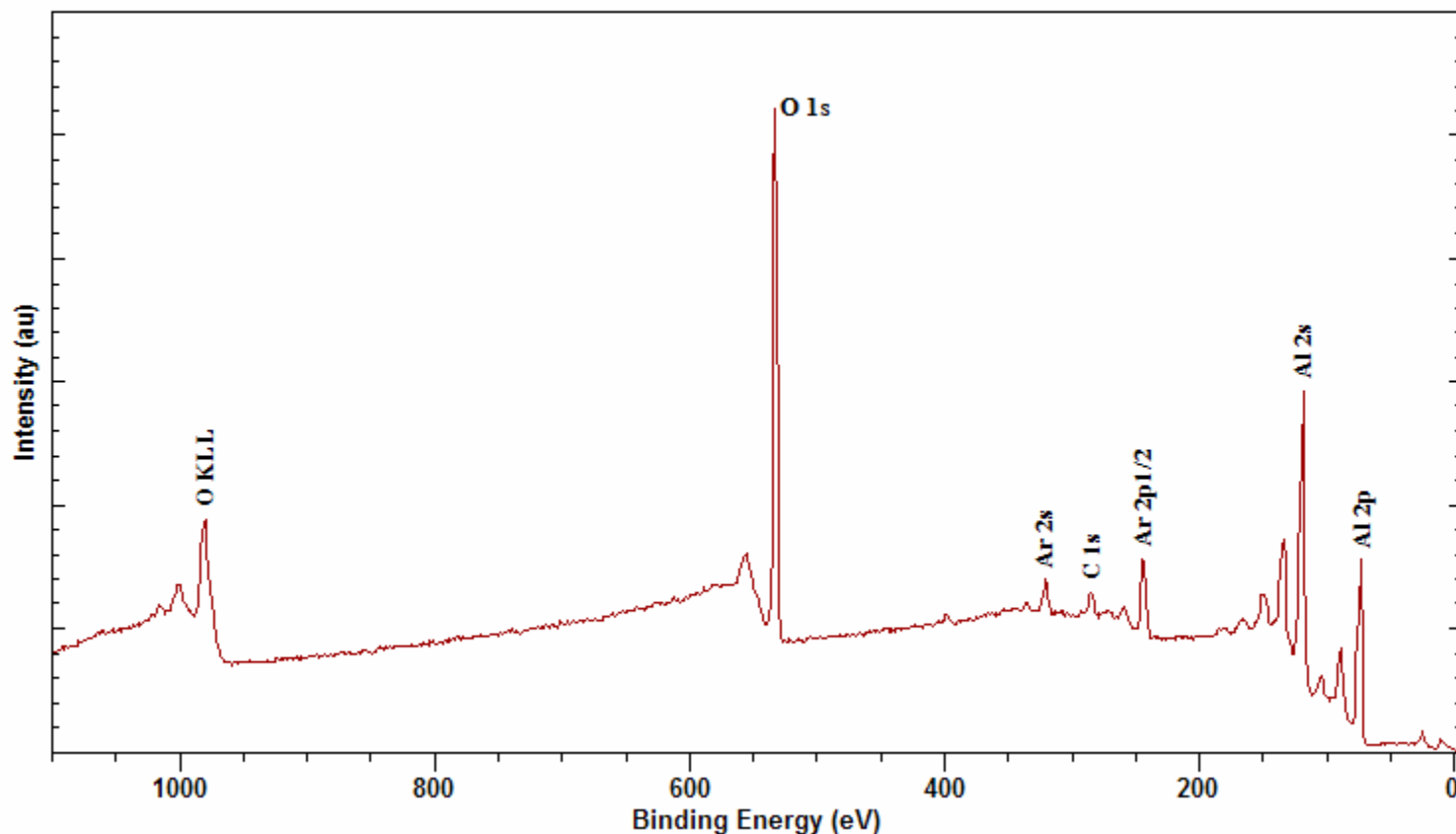


Note the relative movement of the O KLL Auger line relative to the O 1s peak for data acquired using a magnesium anode compared to the SiO₂ data measured with an aluminium anode. The elemental silicon in the sample also accounts for the sequence of plasmon loss peaks not seen in the SiO₂ data.



Aluminium oxide sample analysed using an aluminium monochromatic source.

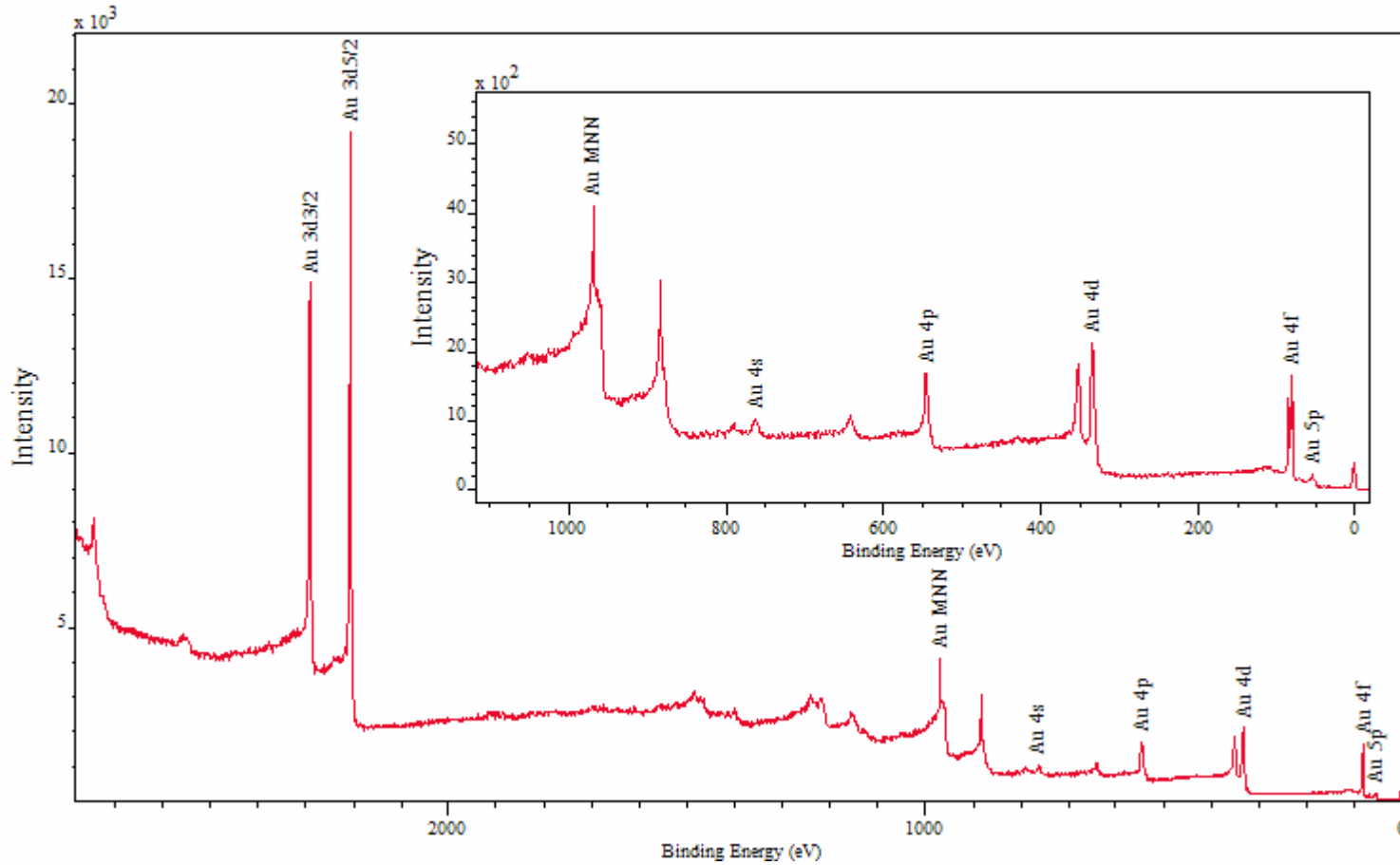
Al Metal & Oxide



Printed using CasaXPS

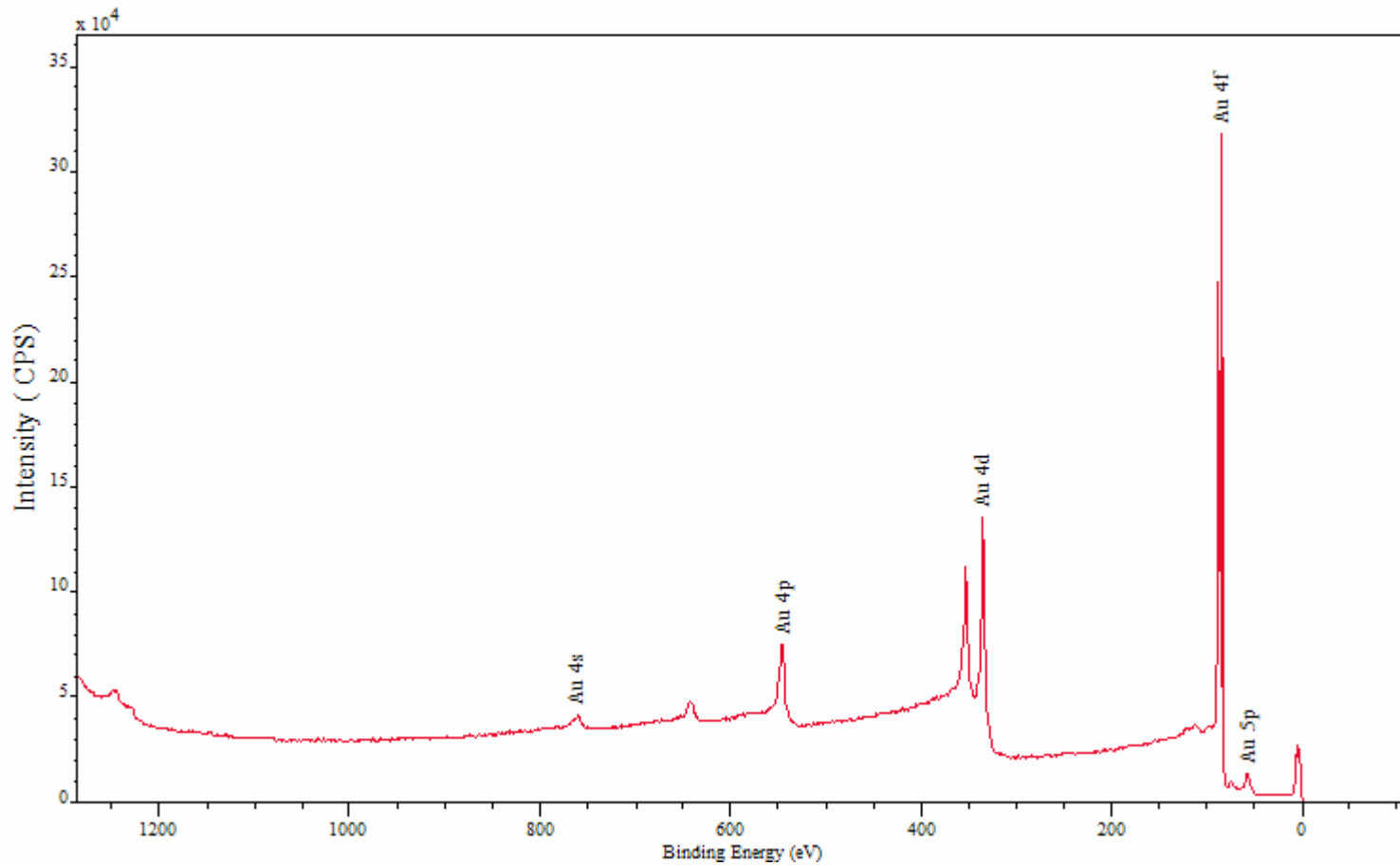
Again, metallic aluminium is responsible for the sequence of plasmon loss peaks associated with the Al 2p and Al 2s photoelectric lines not present in the aluminium oxide spectrum. It is worth observing the argon from the ion gun used to reduce the depth of the aluminium oxide layer exhibits plasmon loss structures characteristic of the aluminium metal. Note also that the plasmon loss peaks from the Al 2p transition will interfere with the Al 2s peak, hence the common practice of using the Al 2p line to quantify samples containing aluminium.

Gold Spectrum Measured with Ag X-ray Source

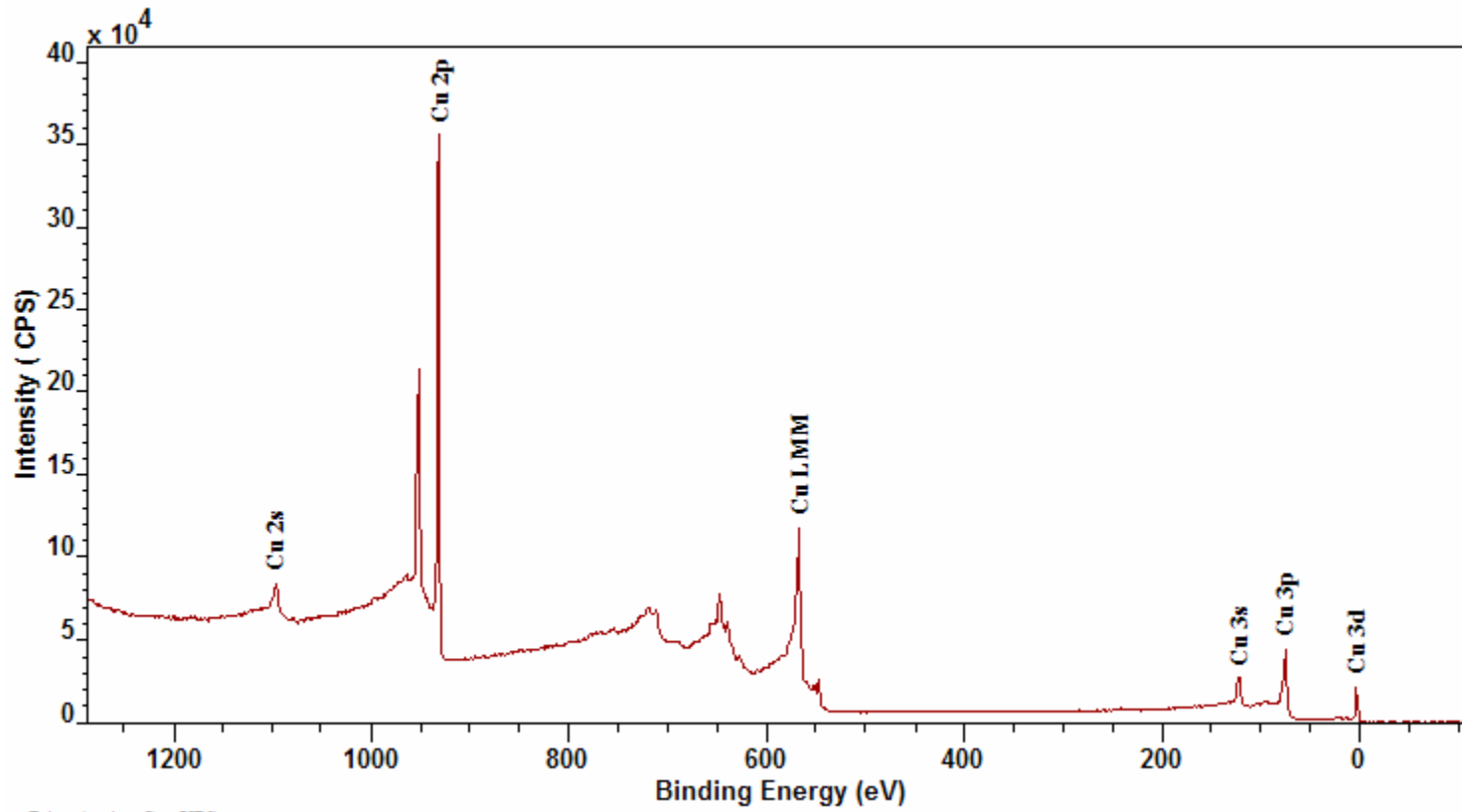


Gold measured using a silver anode in the x-ray monochromatic source.

Gold Measured with Al X-ray Source

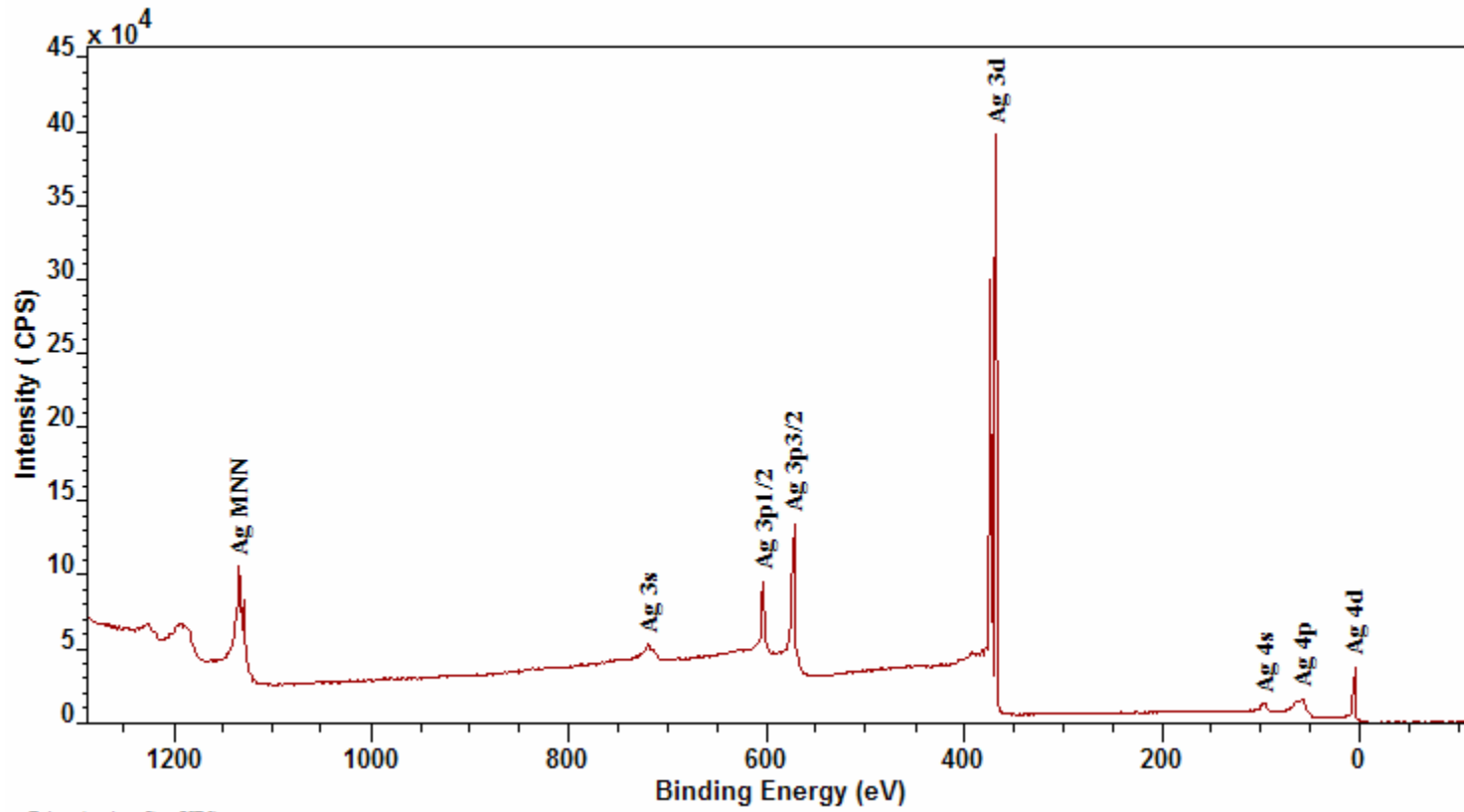


Copper



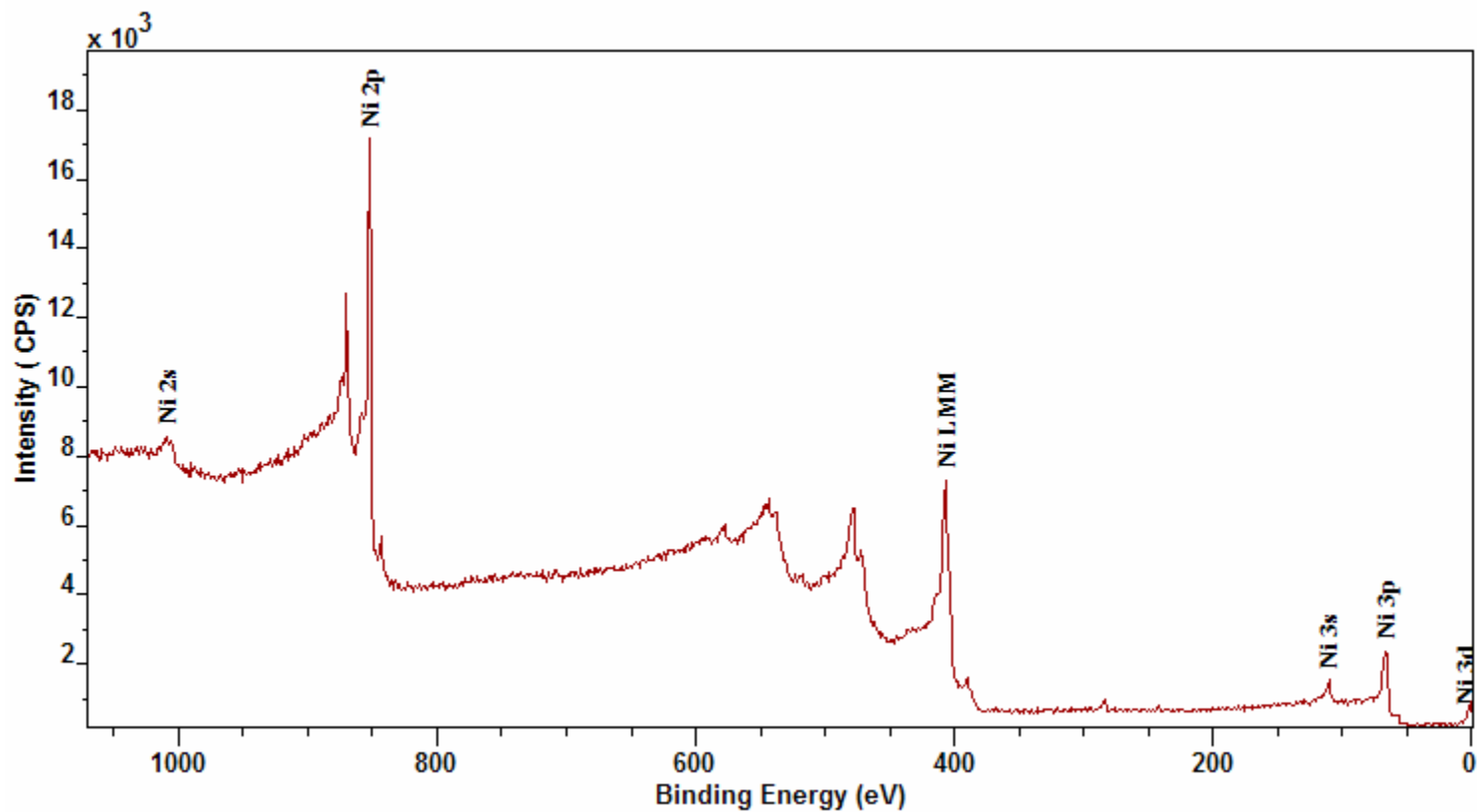
Printed using CasaXPS

Silver



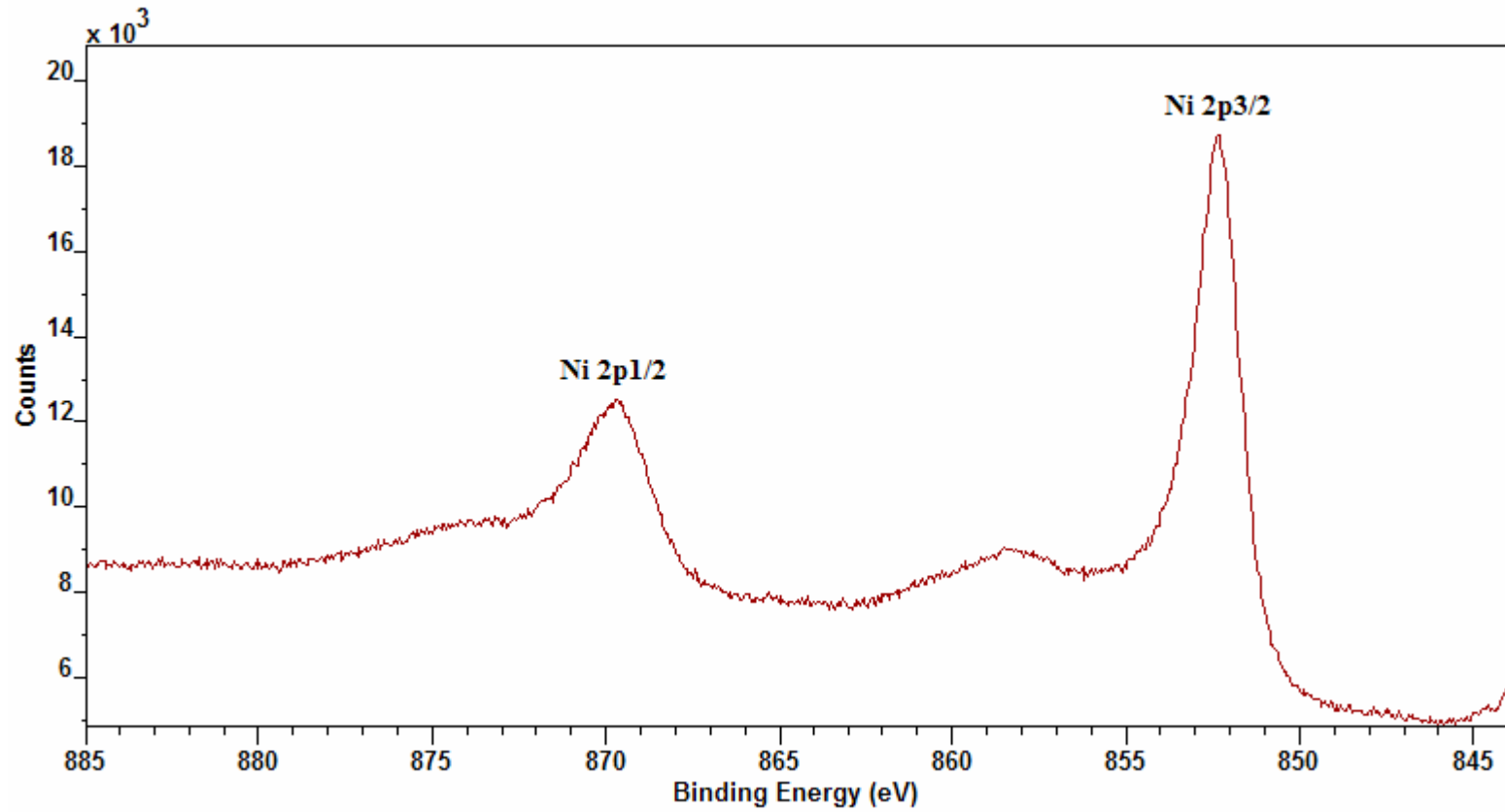
Printed using CasaXPS

Nickel



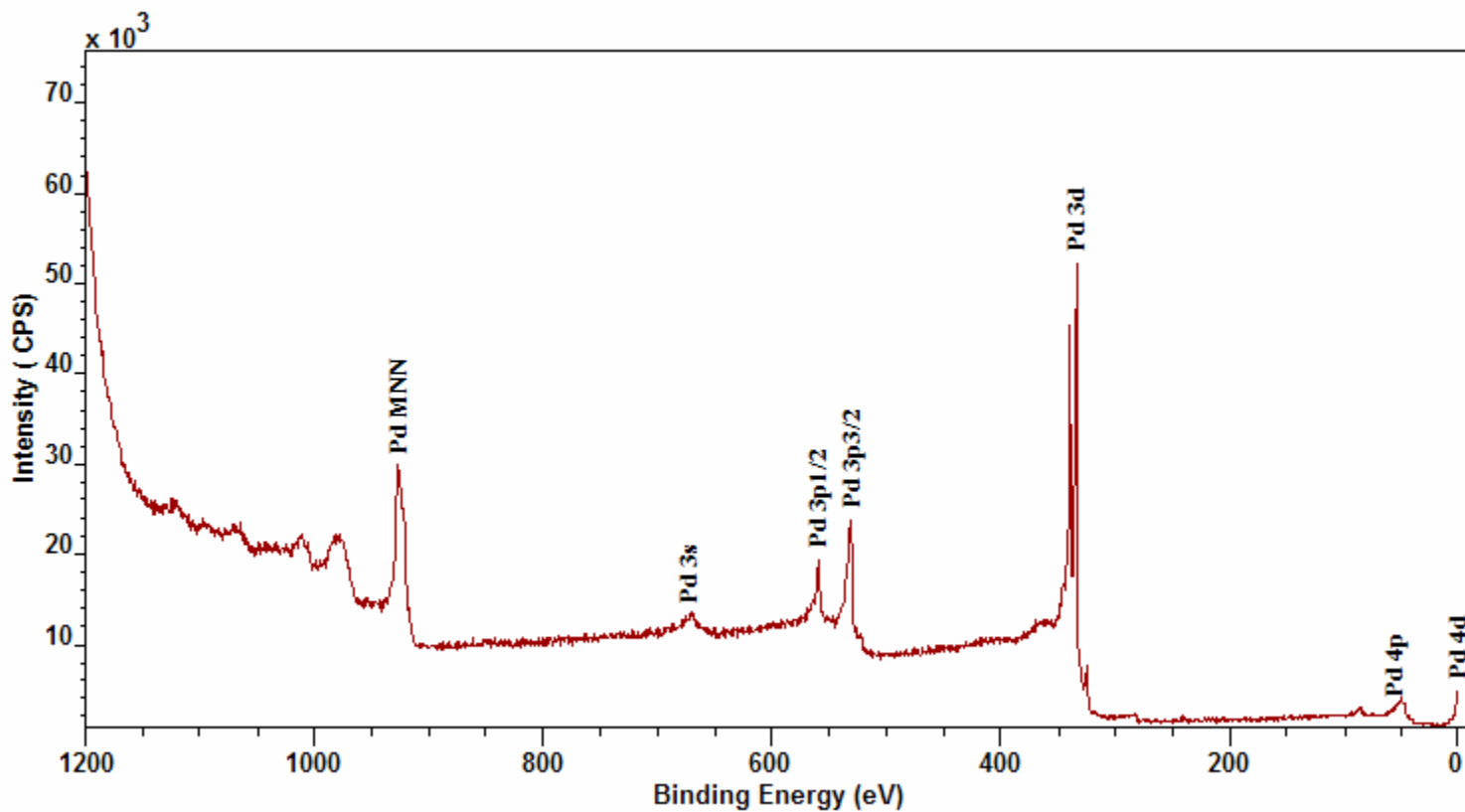
Printed using CasaXPS

Ni 2p



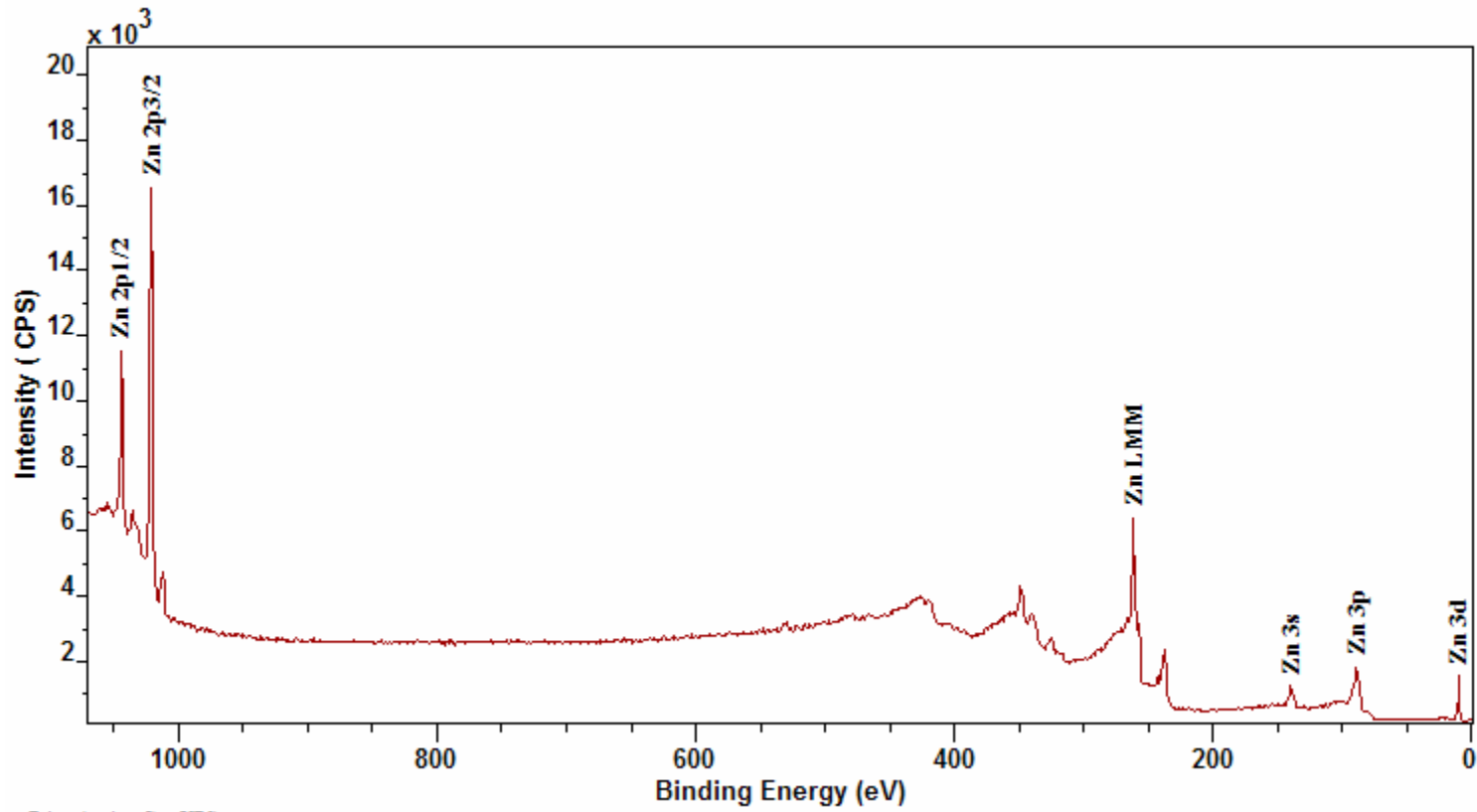
Printed using CasaXPS

Palladium

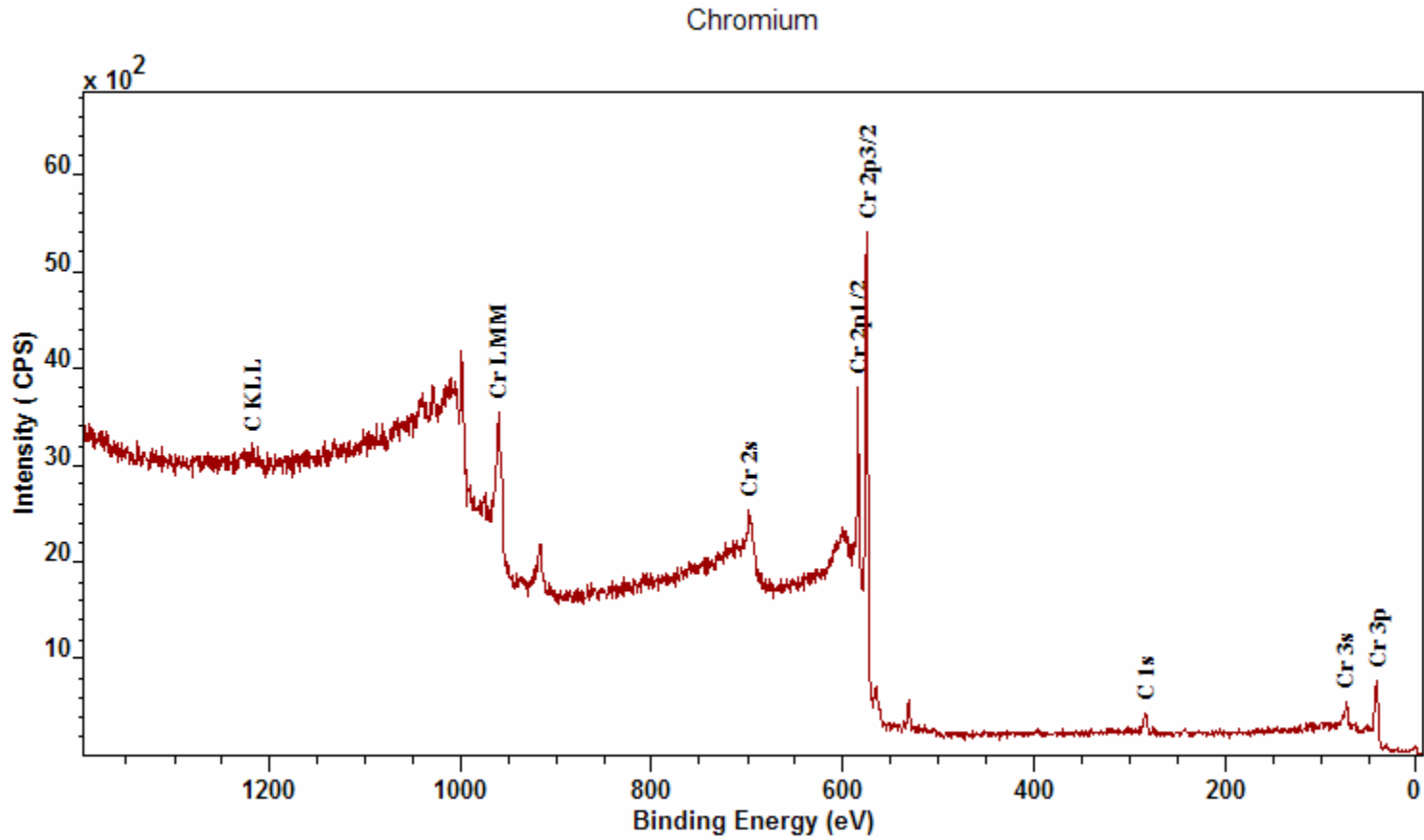


Printed using CasaXPS

Zinc

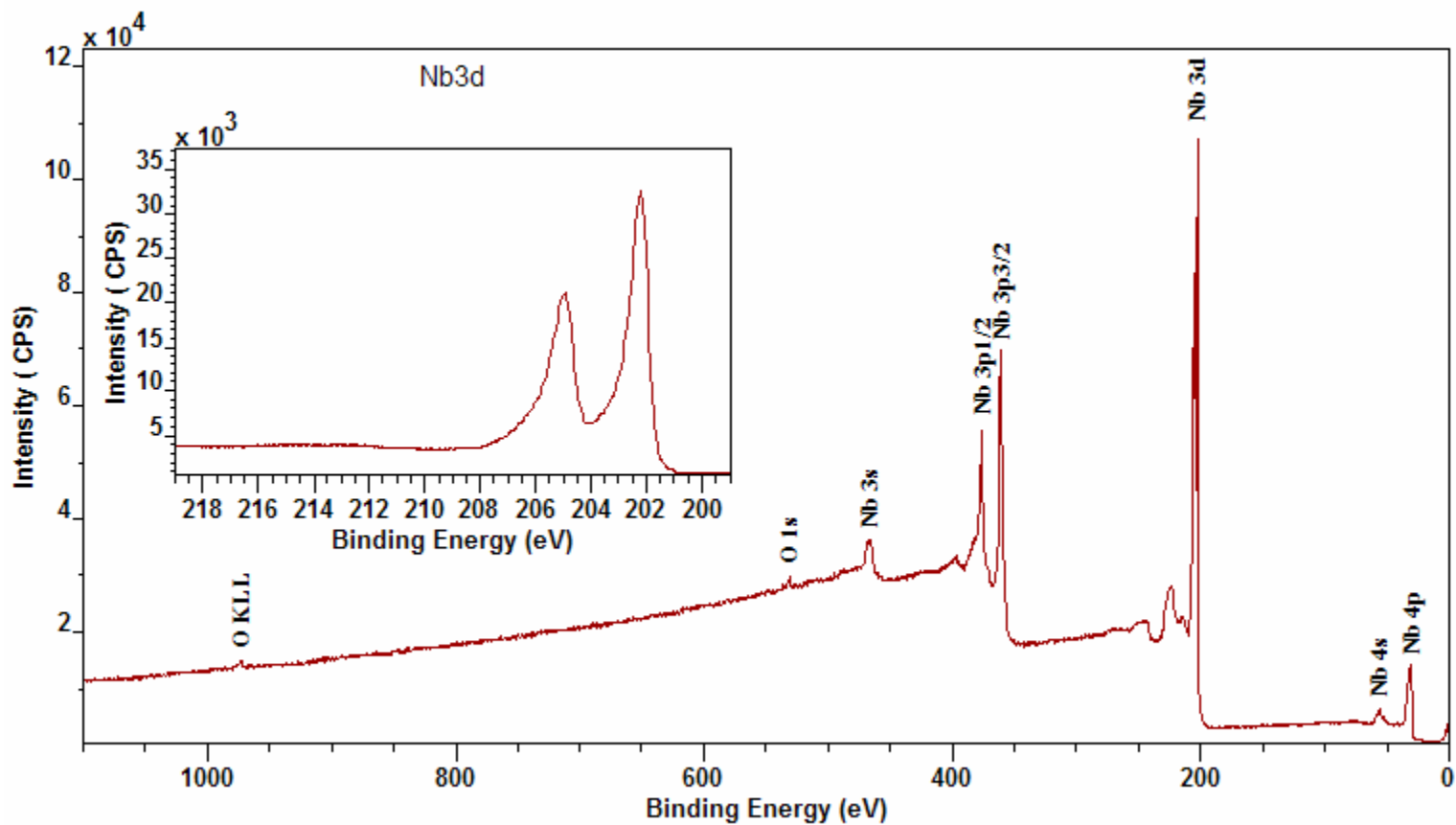


Printed using CasaXPS



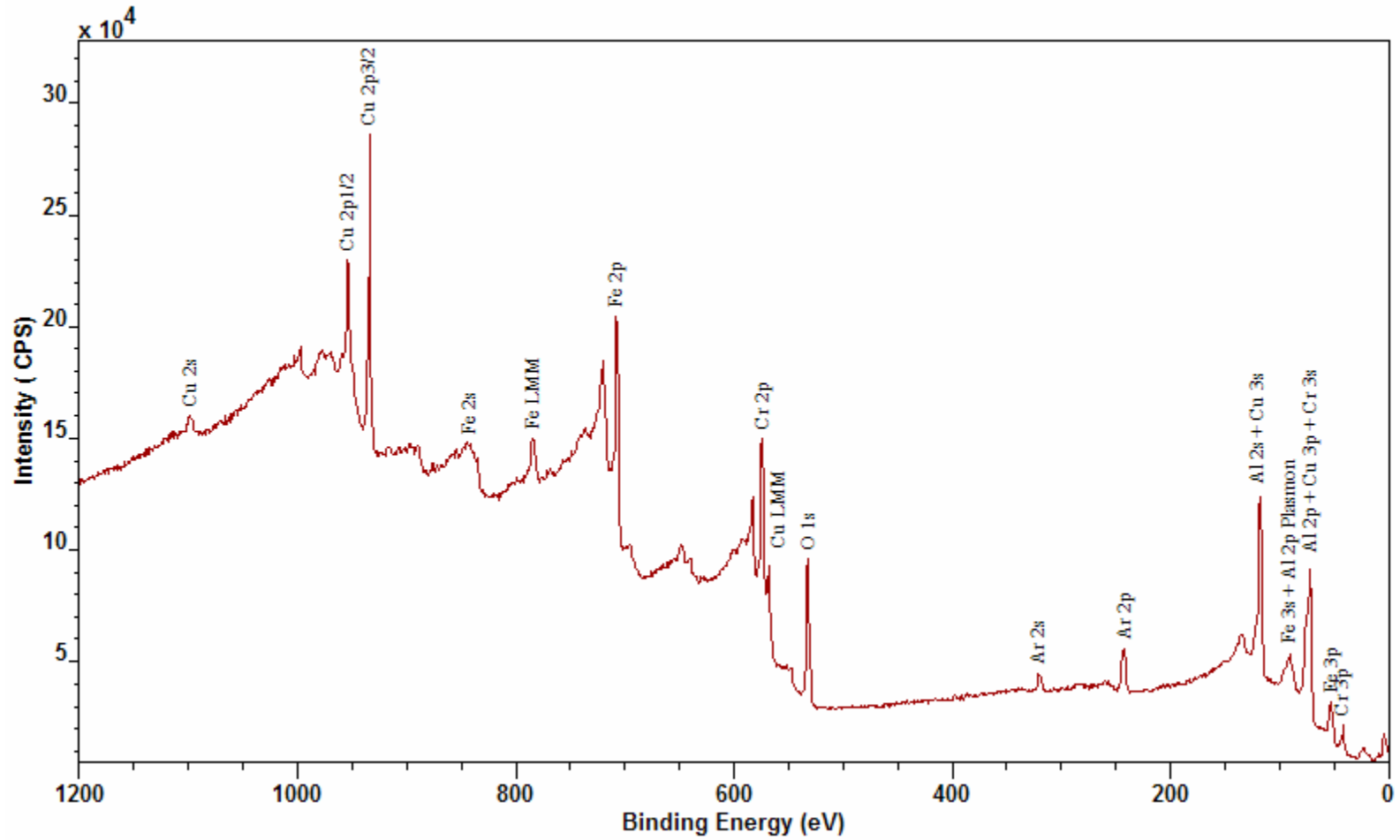
Printed using CasaXPS

Niobium

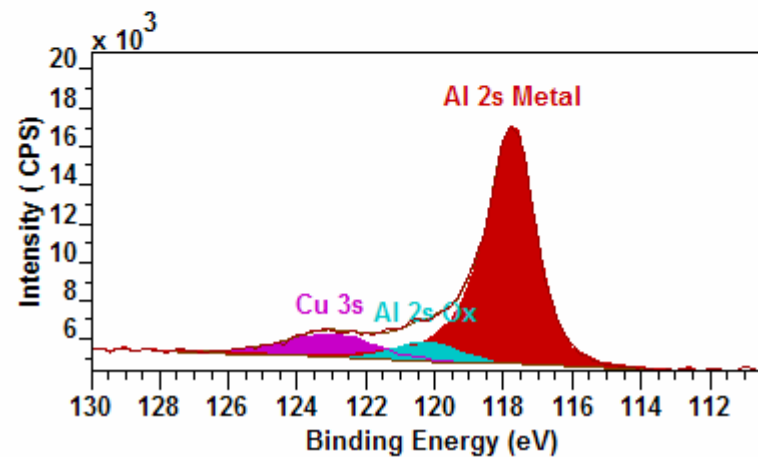
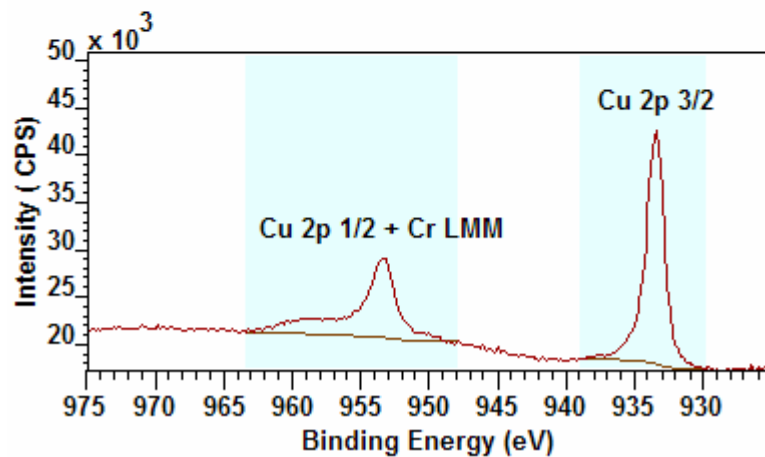
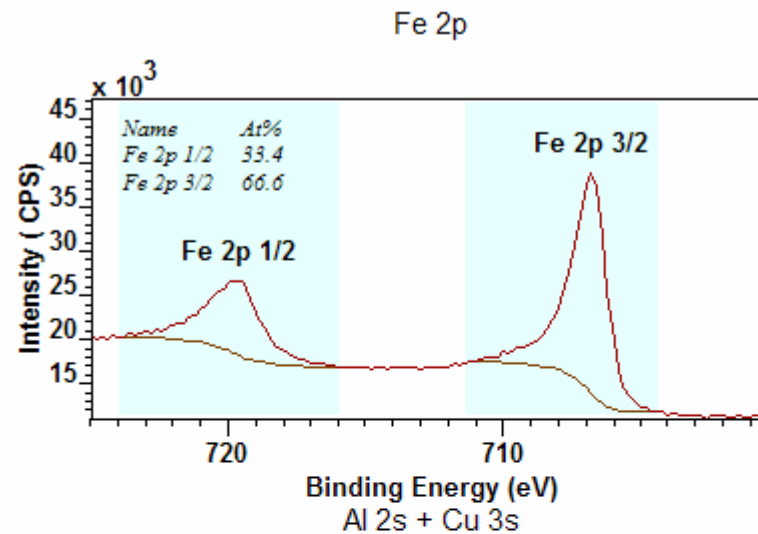
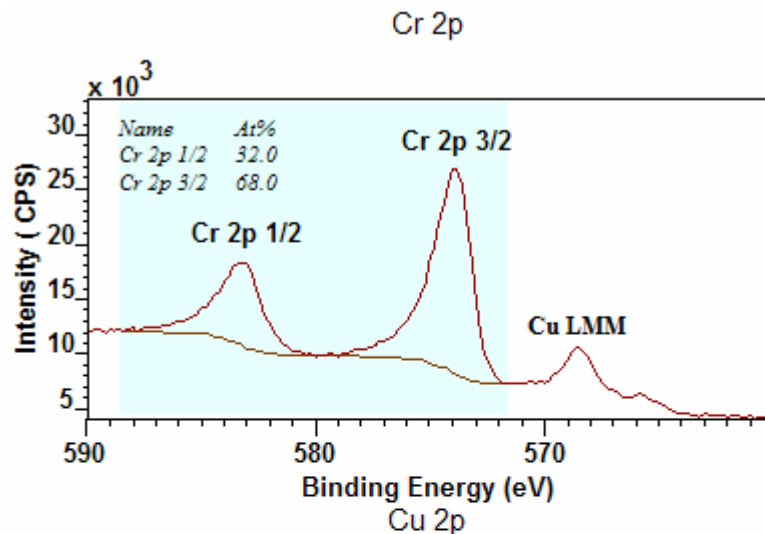


Printed using CasaXPS

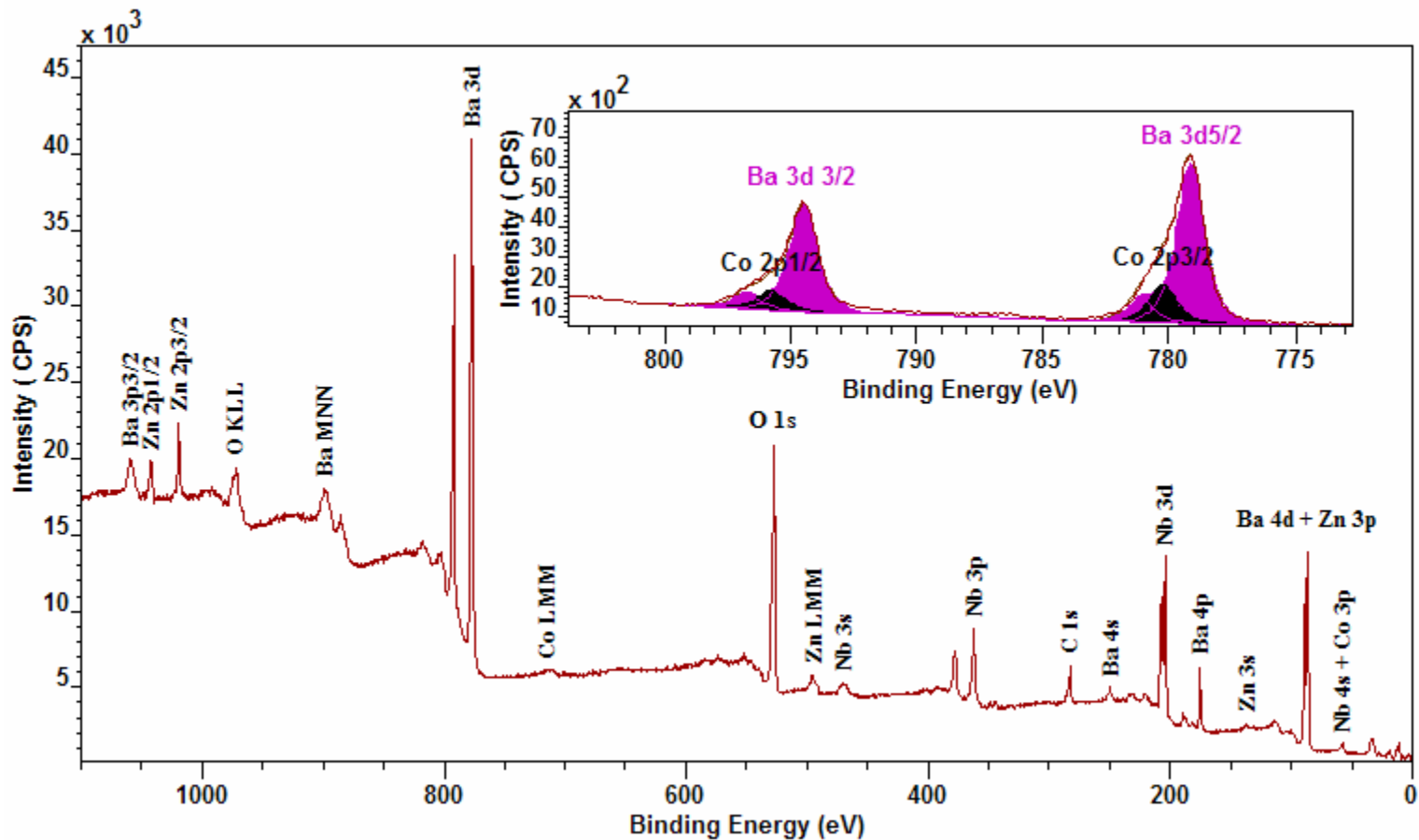
AlCuFeCr quasicrystal



Printed using CasaXPS

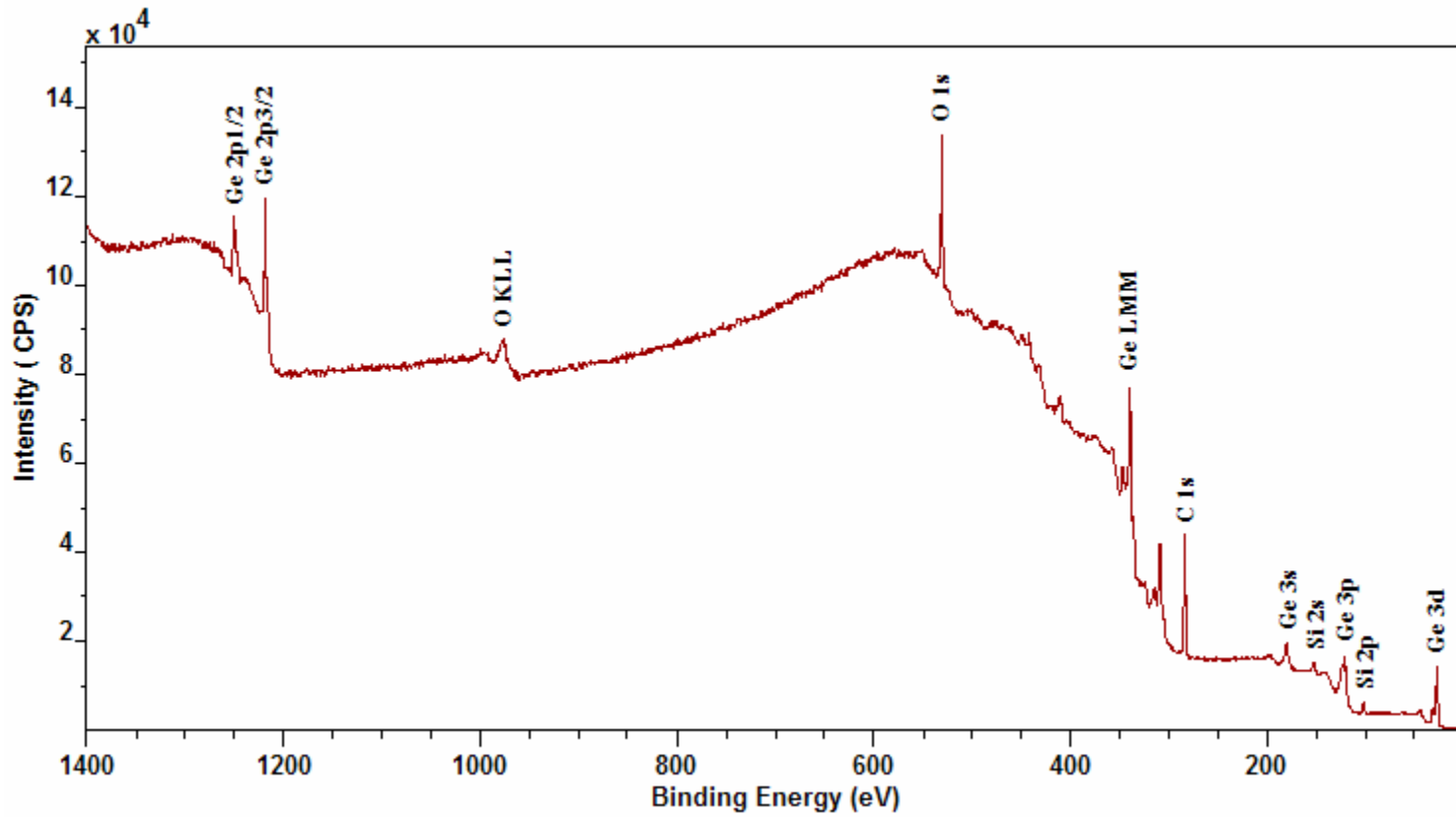


BaCoNb

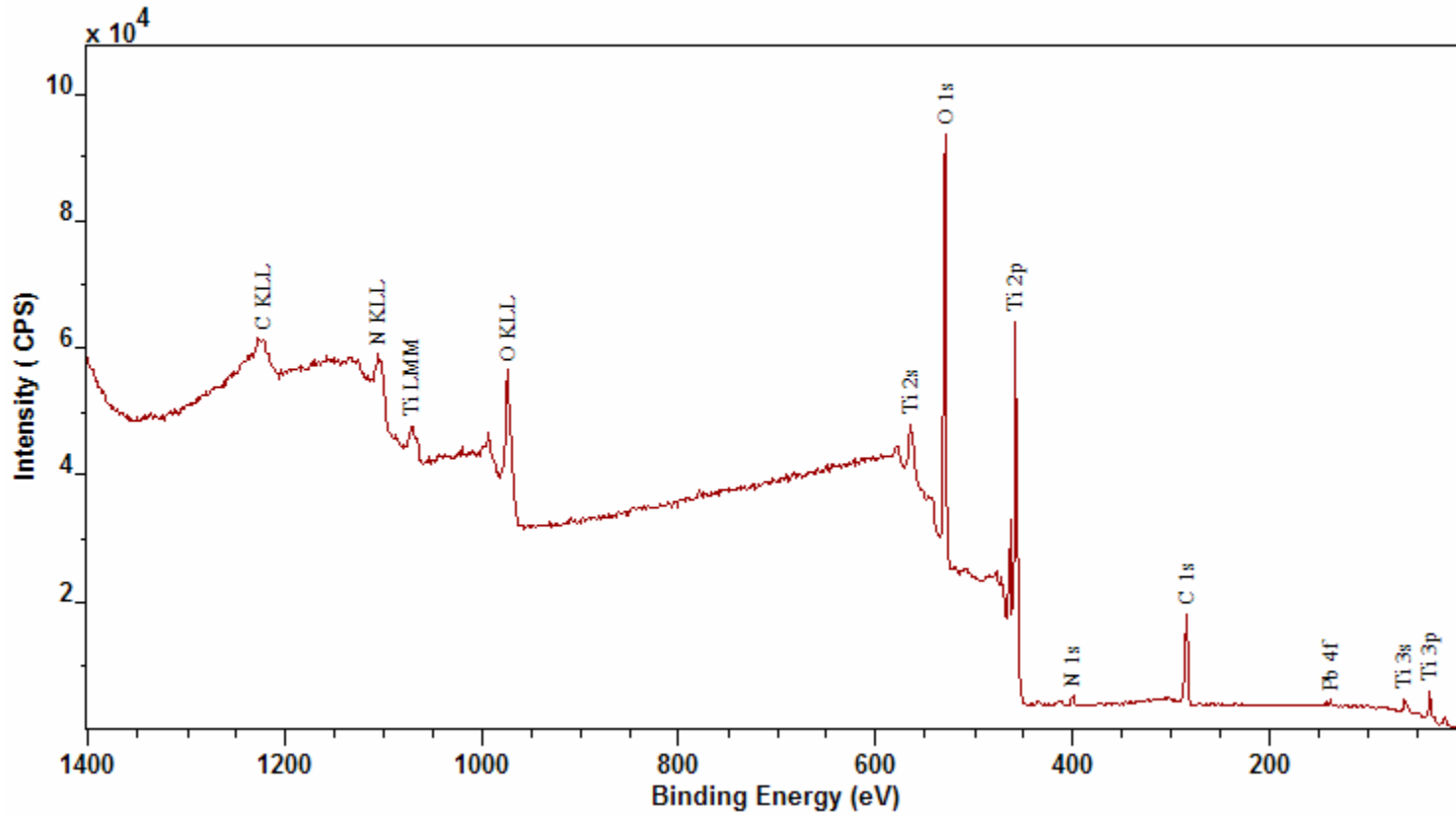


Printed using CasaXPS

Germanium Oxide

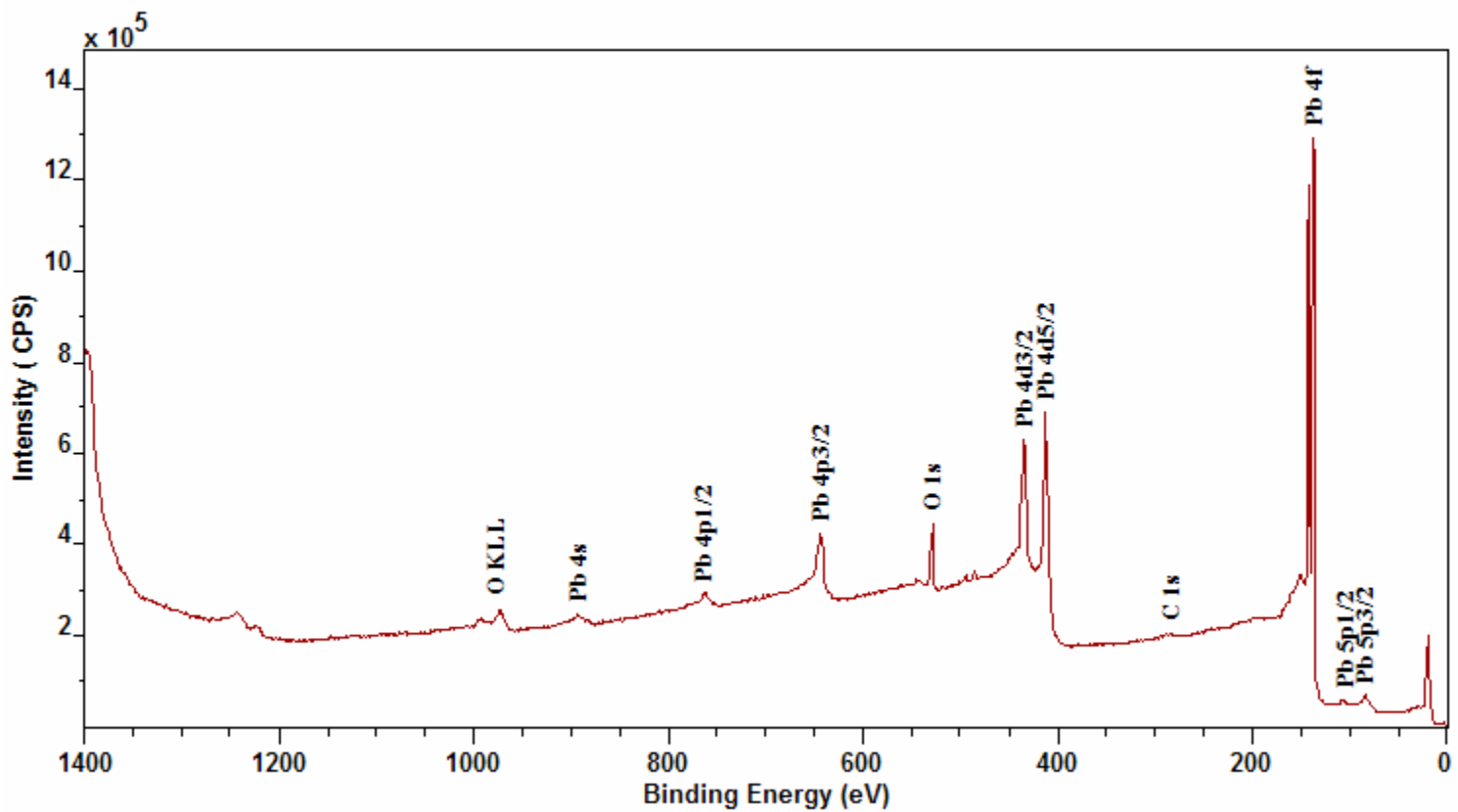


Titanium Oxide



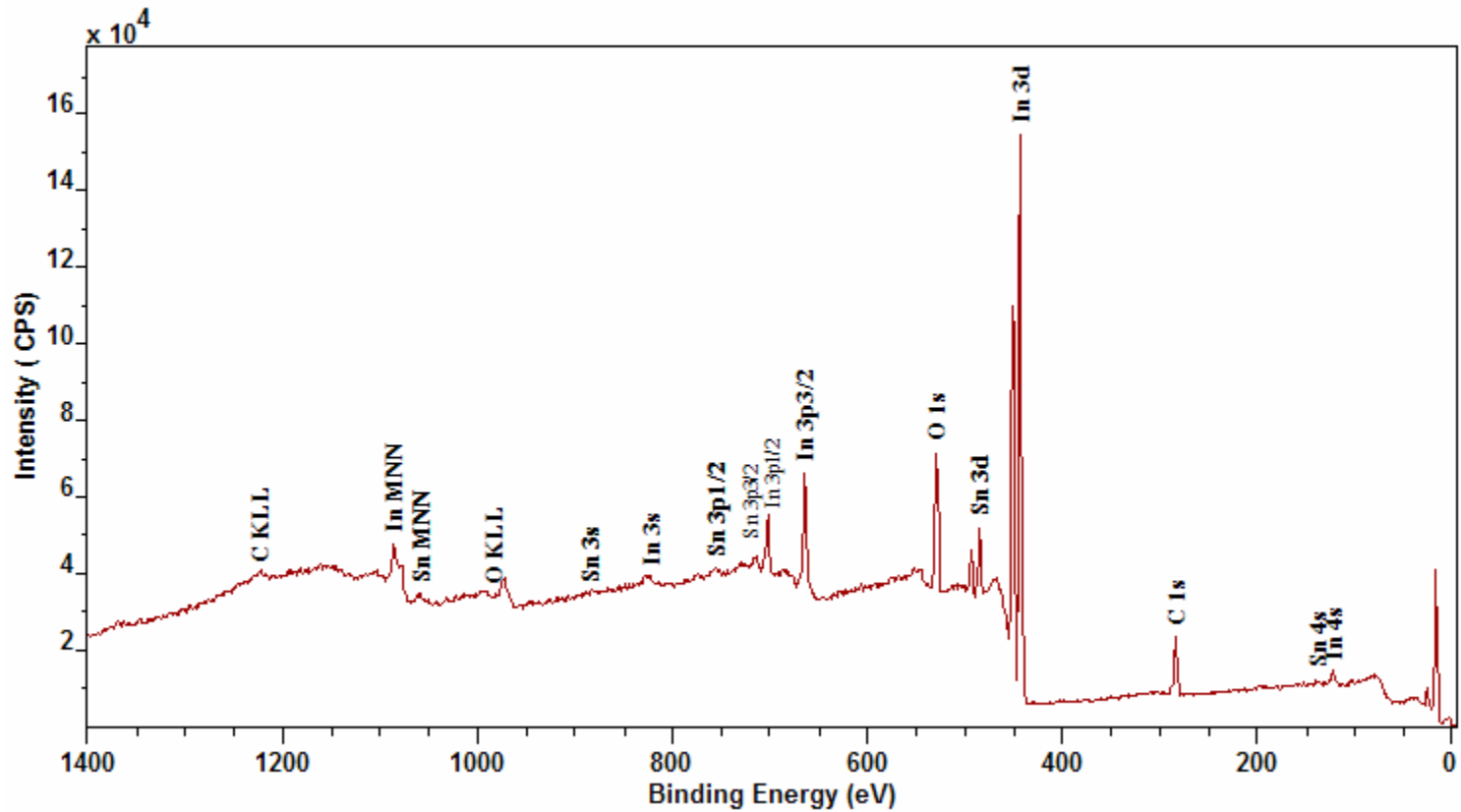
Printed using CasaXPS

Lead Oxide



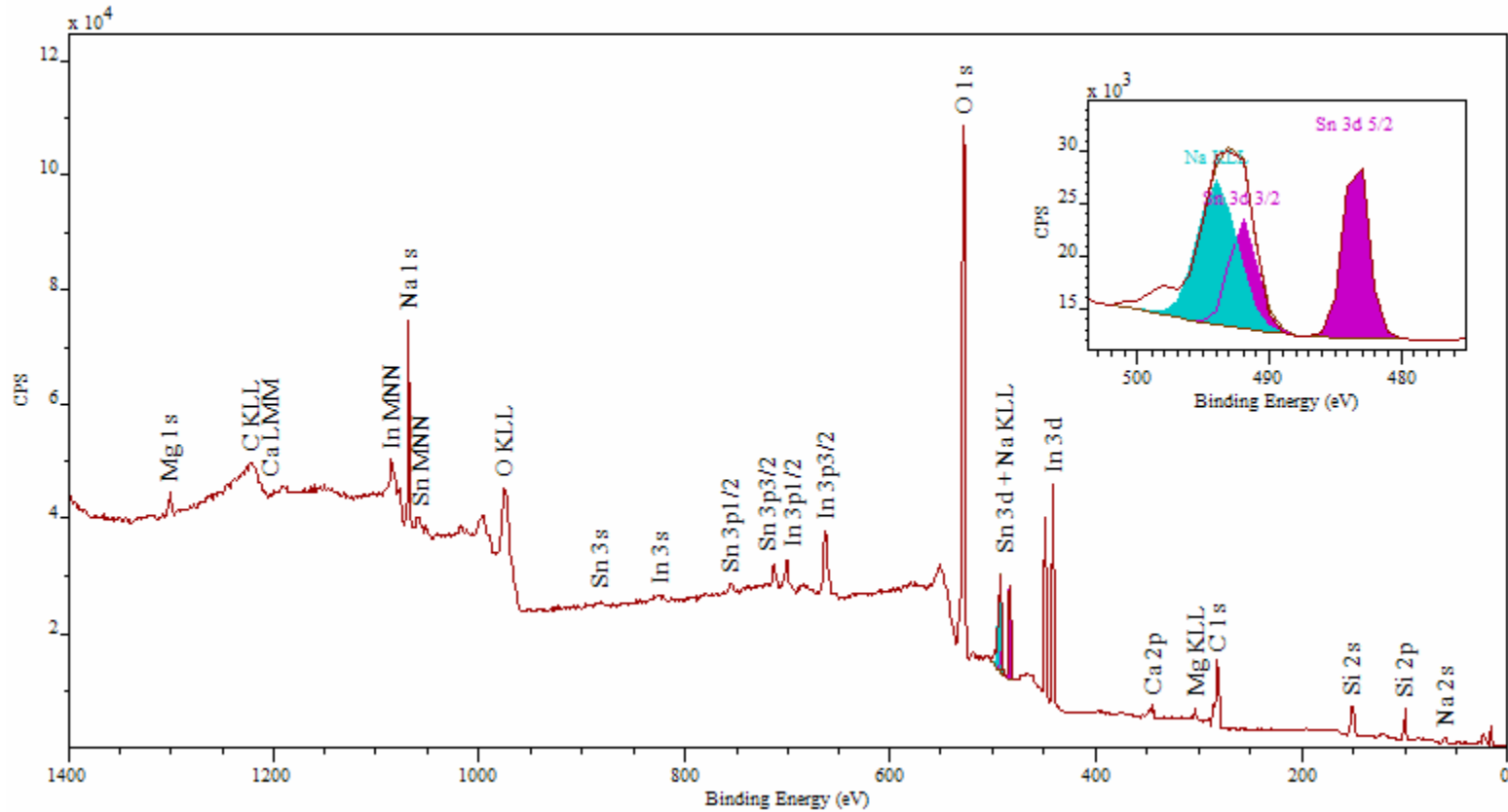
Printed using CasaXPS

Tin Indium Oxide

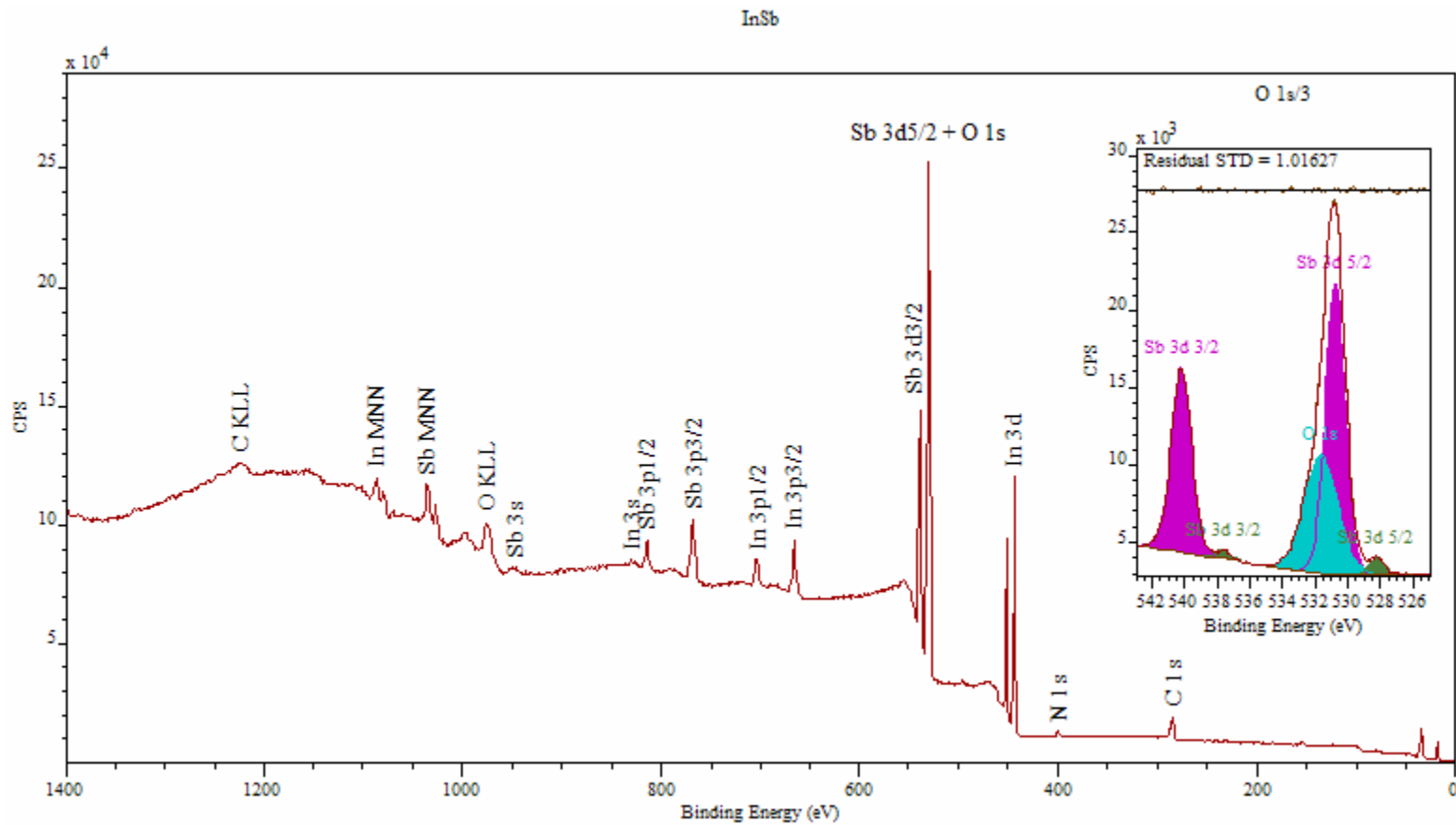


Printed using CasaXPS

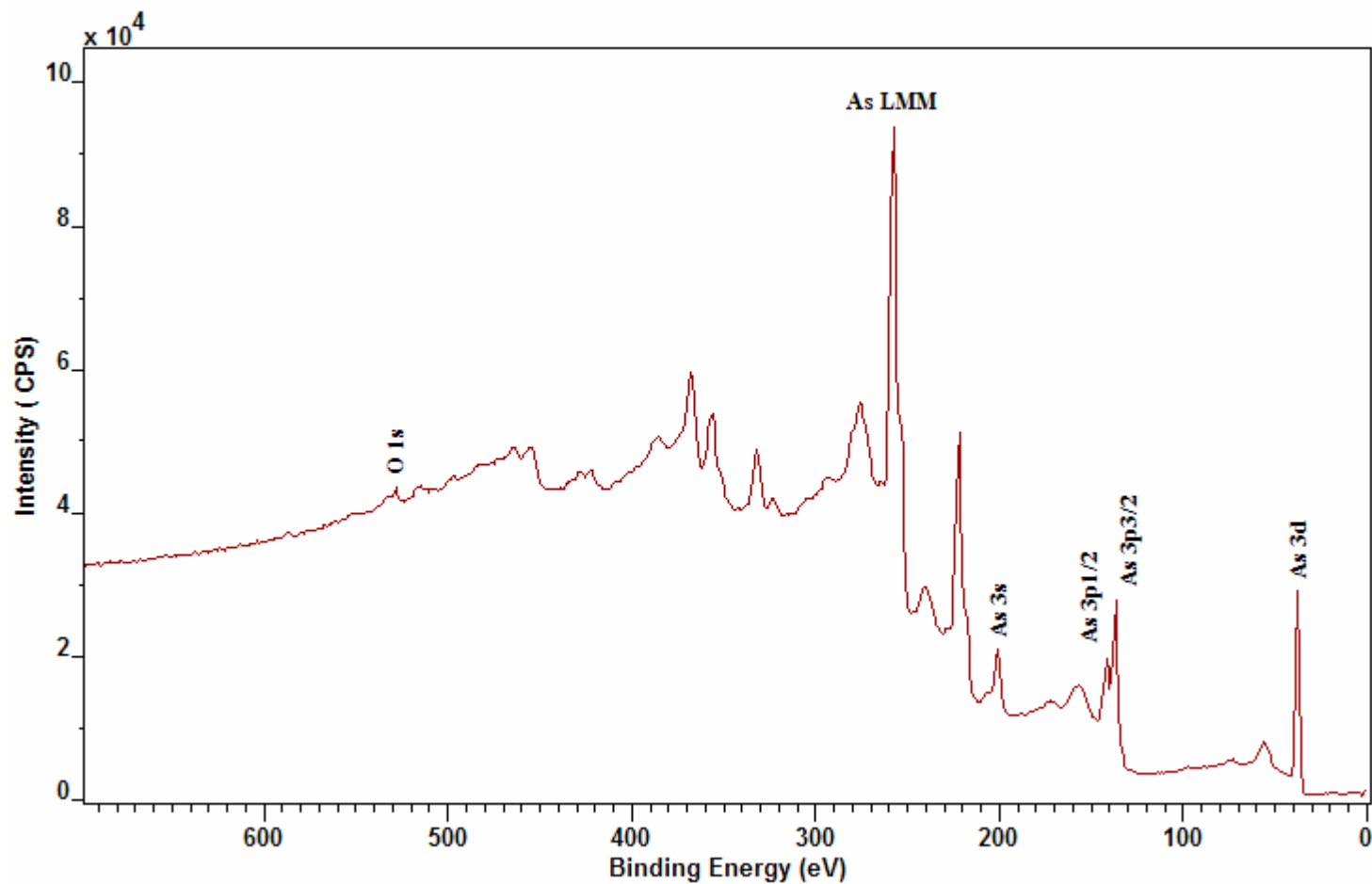
ITO Glass



Printed using CasaXPS

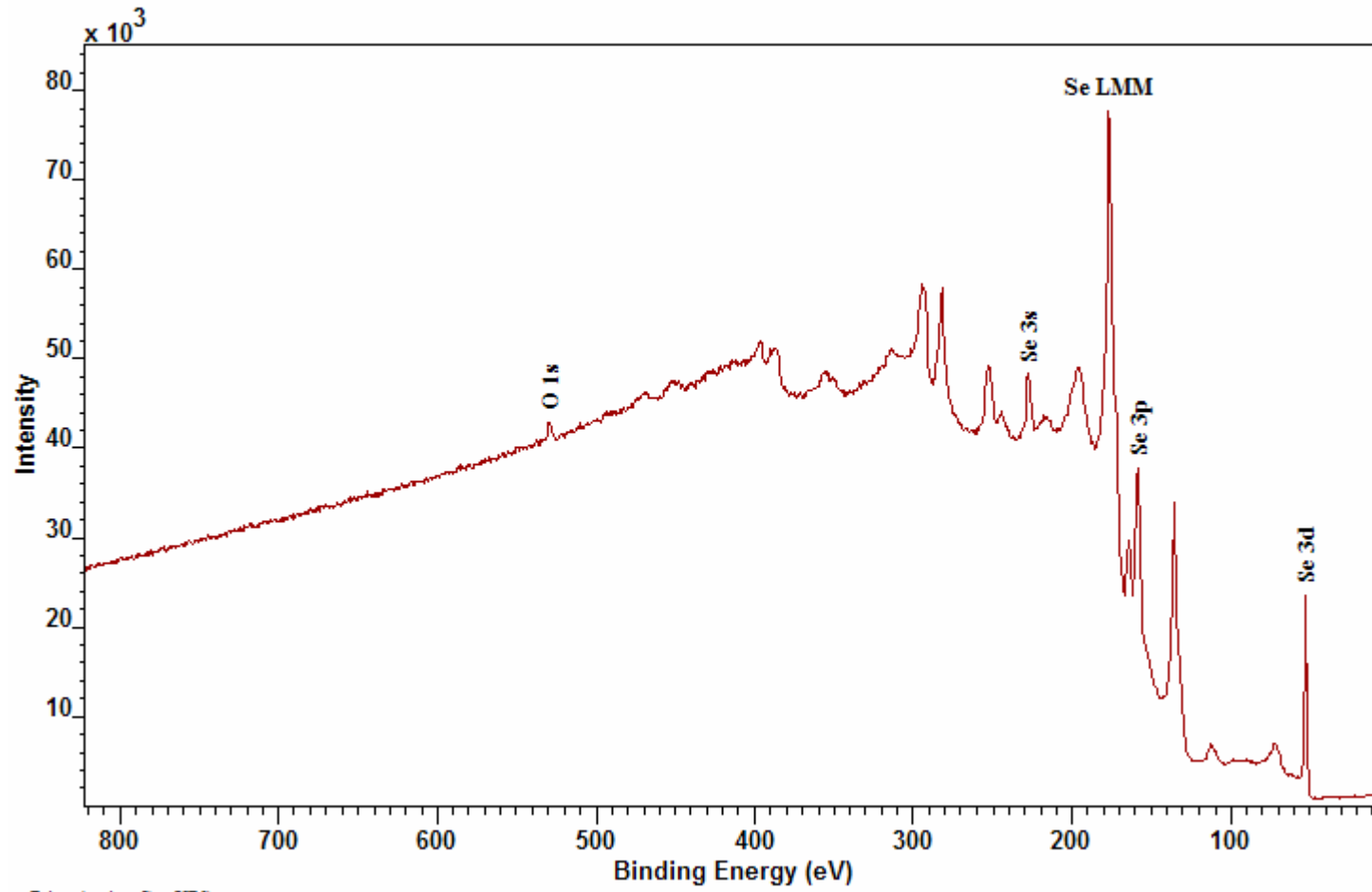


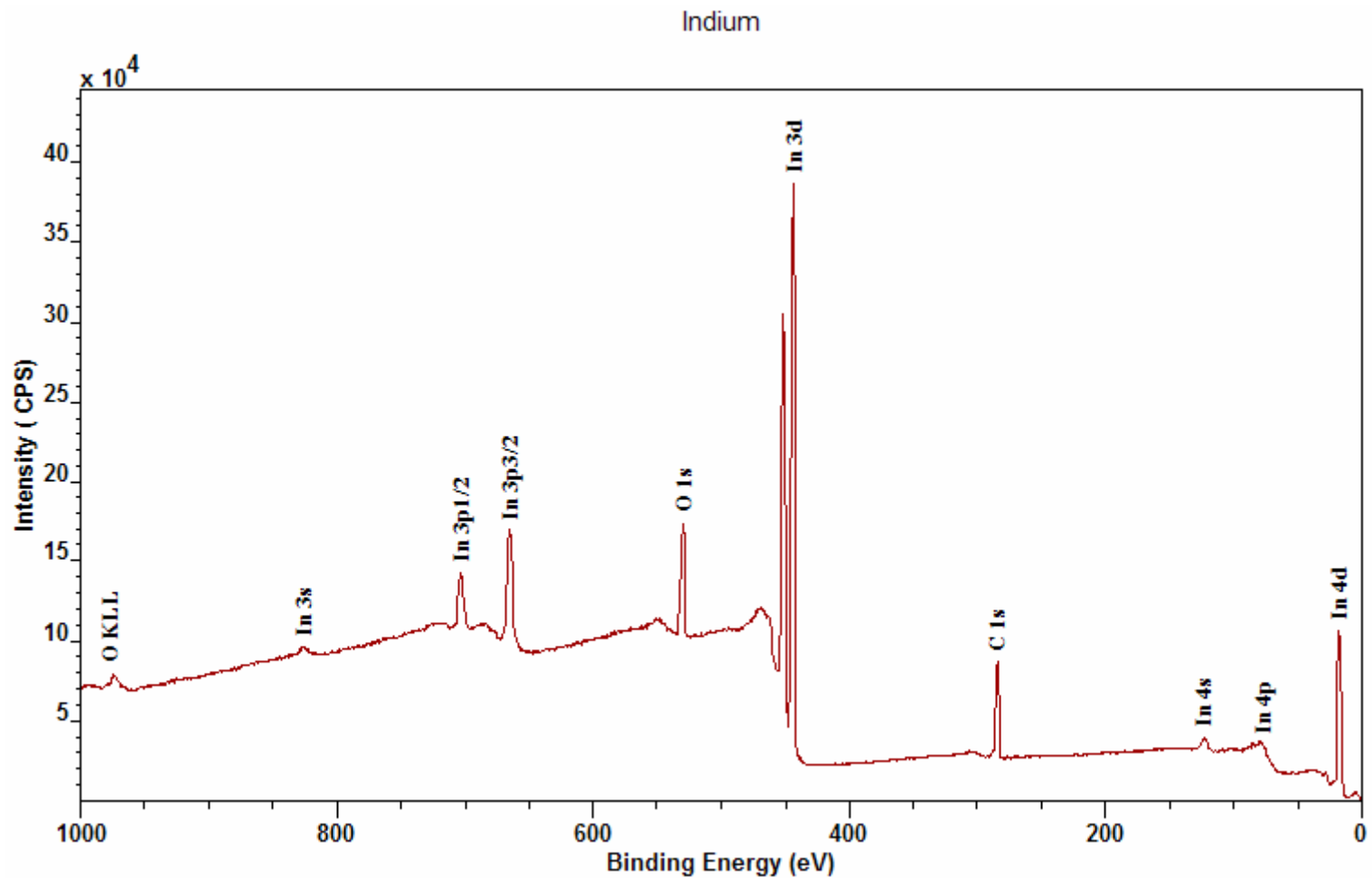
Arsenic



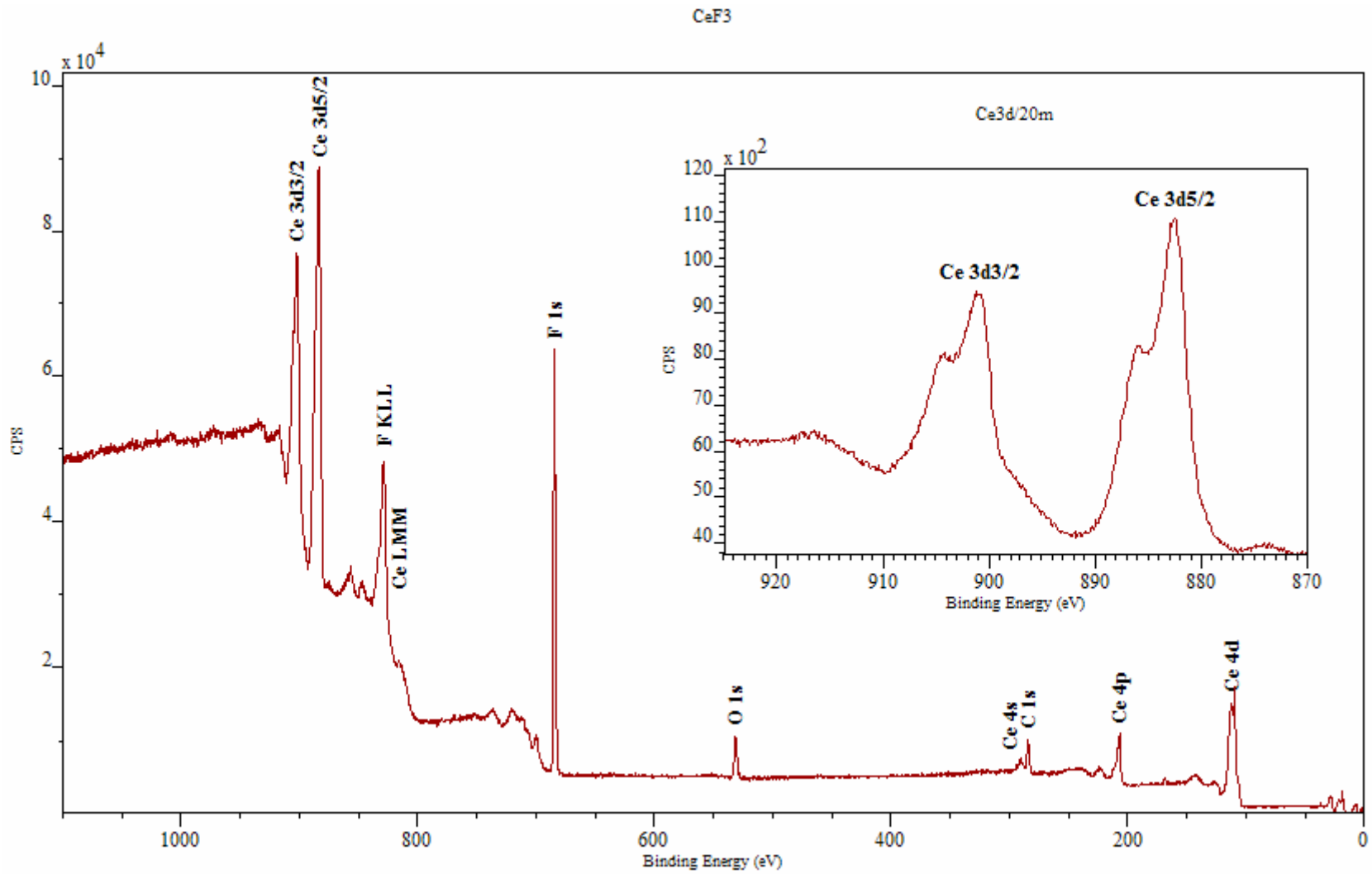
Printed using CasaXPS

Selenium

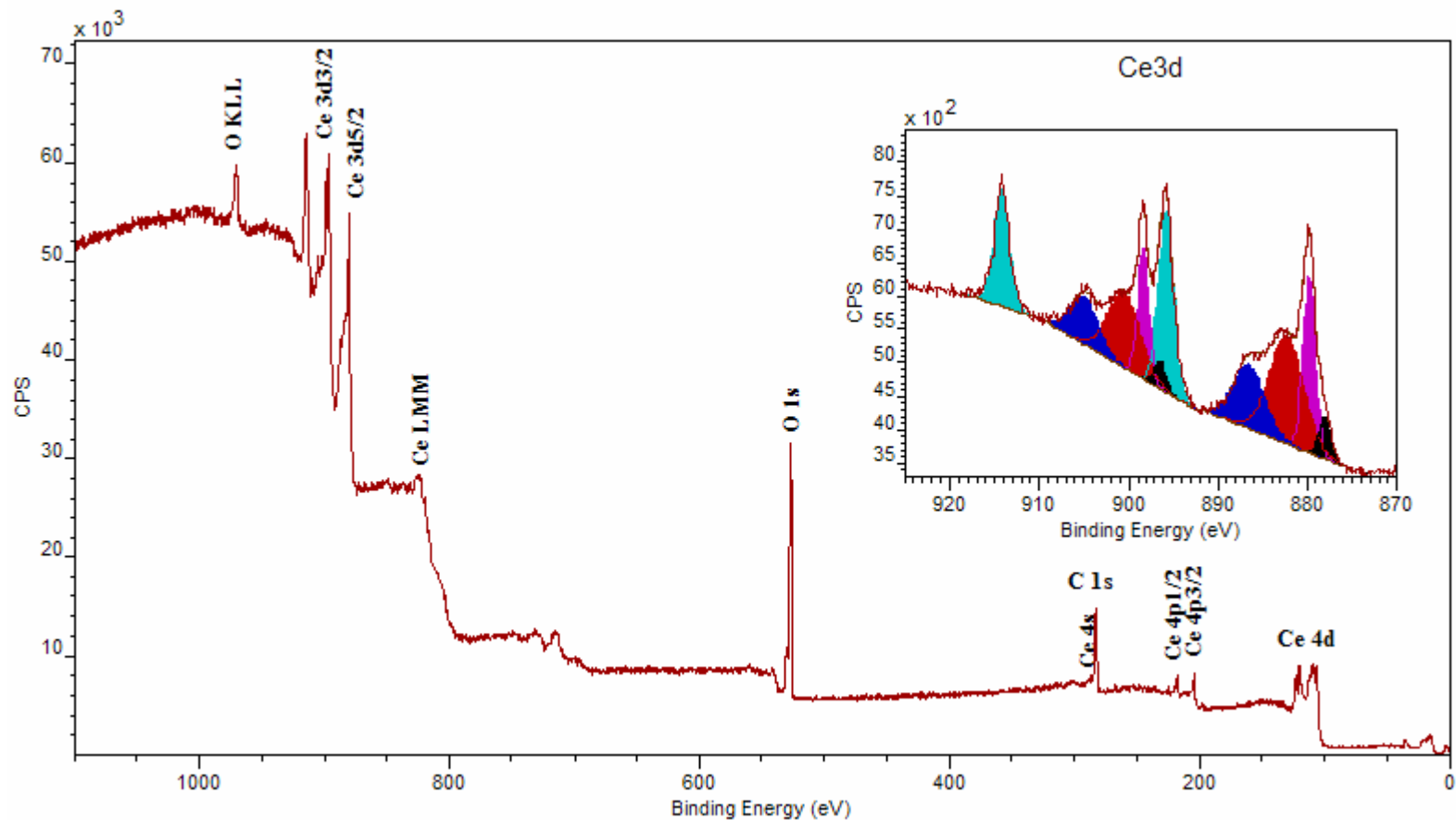




Printed using CasaXPS



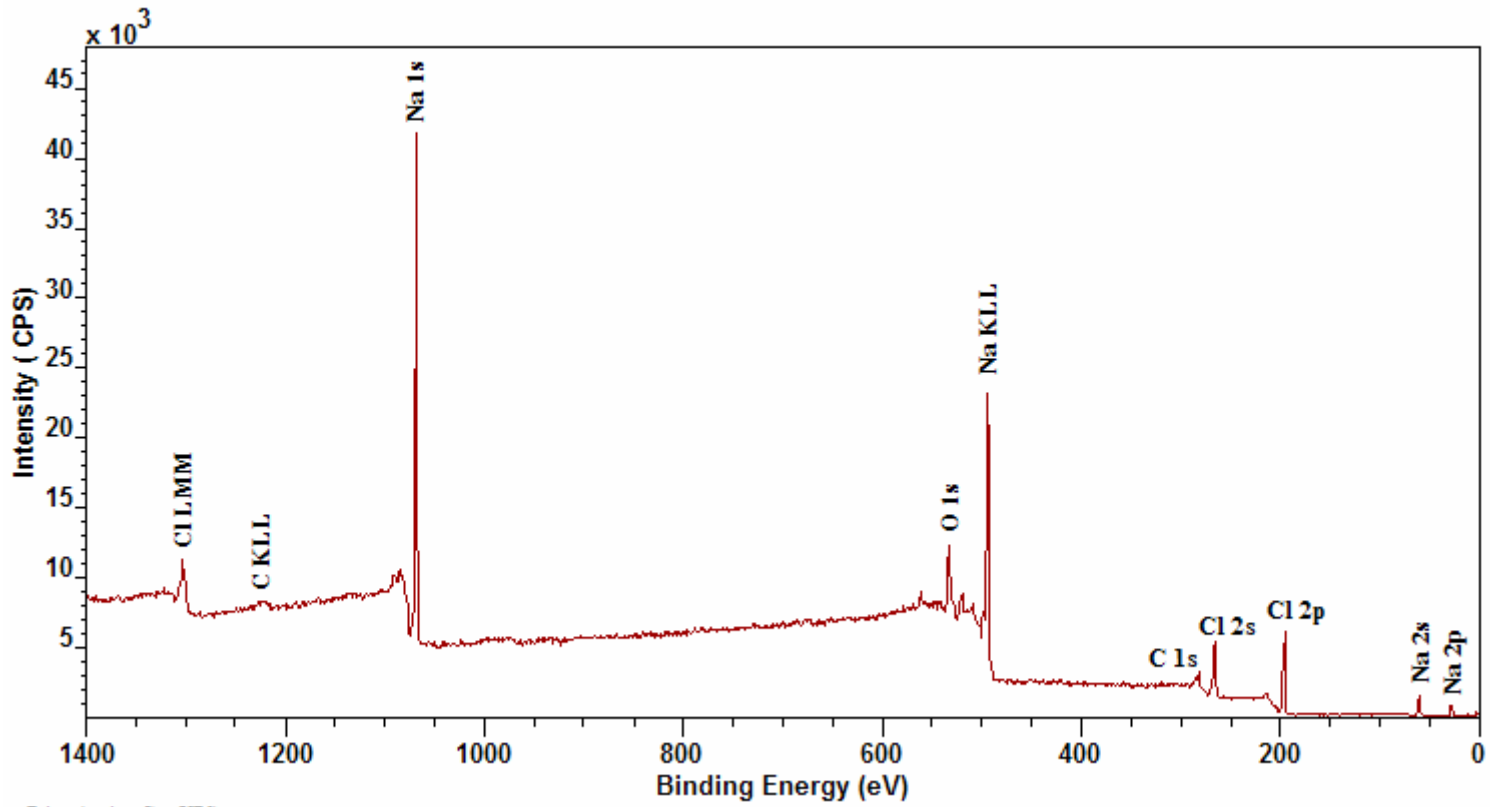
Ce Oxide



Printed using CasaXPS

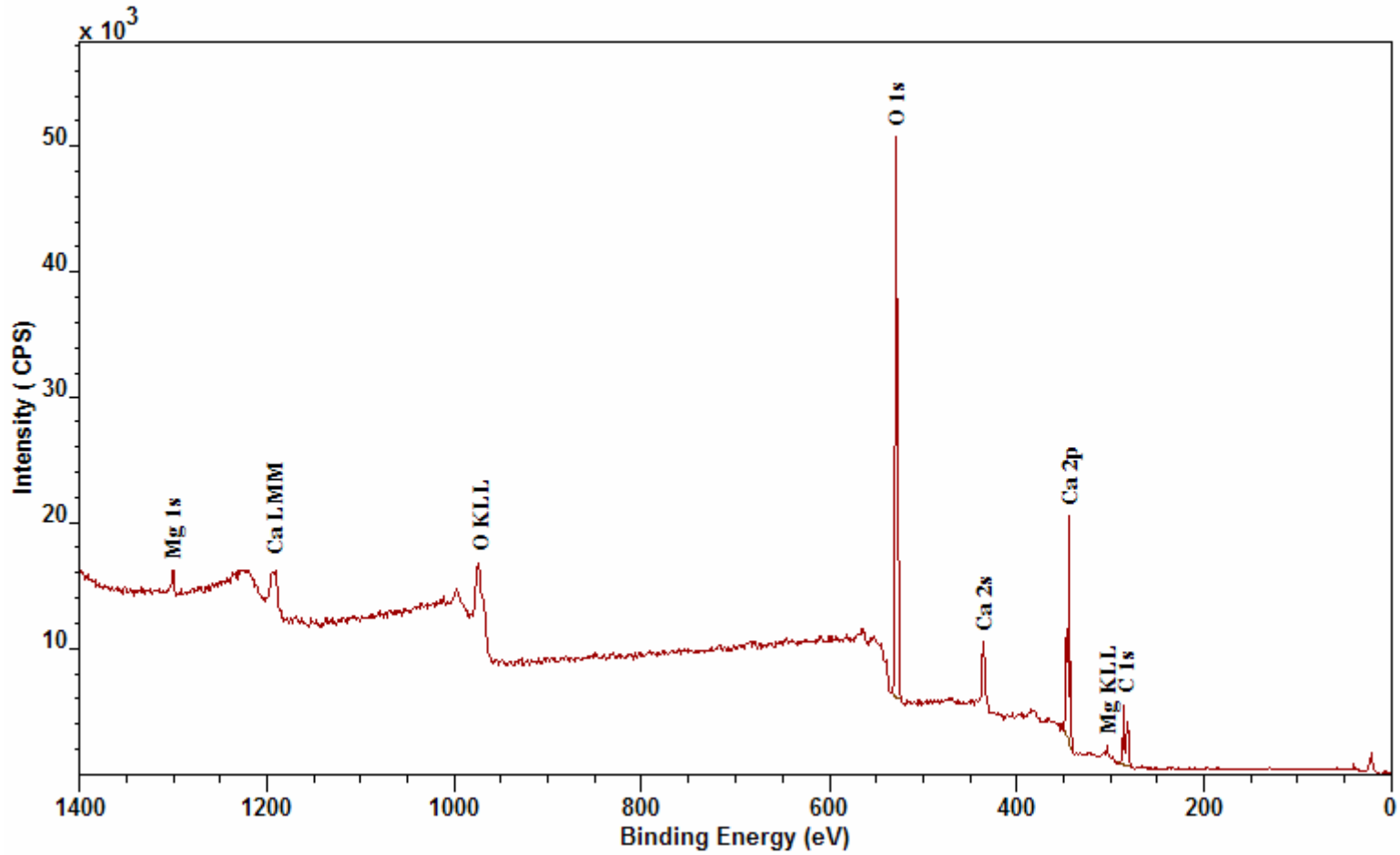
The peak model is to illustrate a complex data envelope fitted with simple Gaussian-Lorentzian lineshapes. For a more complete discussion of Ce Oxide please see: V. Matolín, M. Cabala, V. Cháb, I. Matolínová, K. C. Prince, M. Škoda, F. Šutara, T. Skála and K. Veltruská, A resonant photoelectron spectroscopy study of Sn(Ox) doped CeO₂ catalysts, *Surf. Interface Anal.* 40 (2008) 225–230.

NaCl



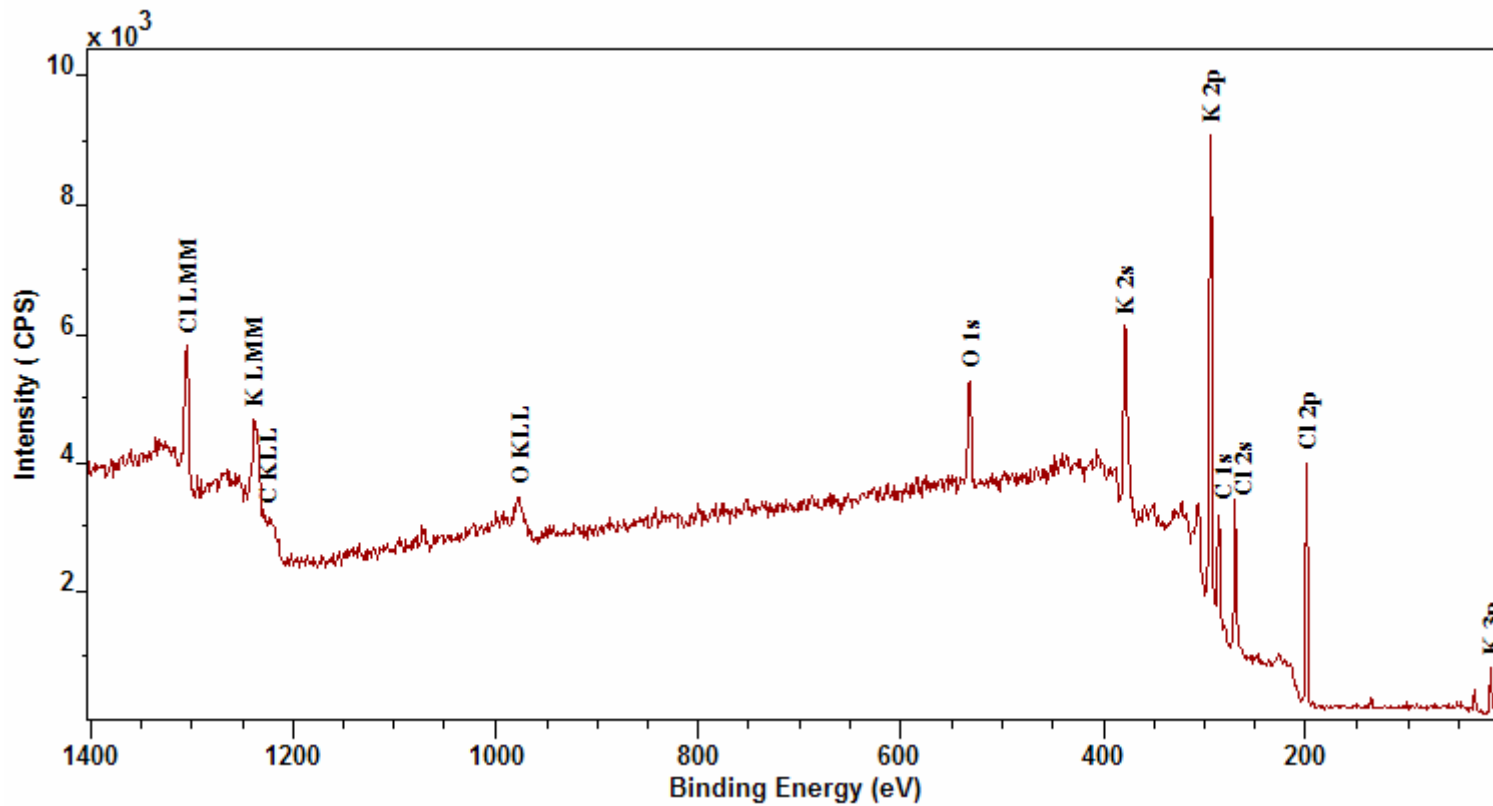
Printed using CasaXPS

CaCO₃



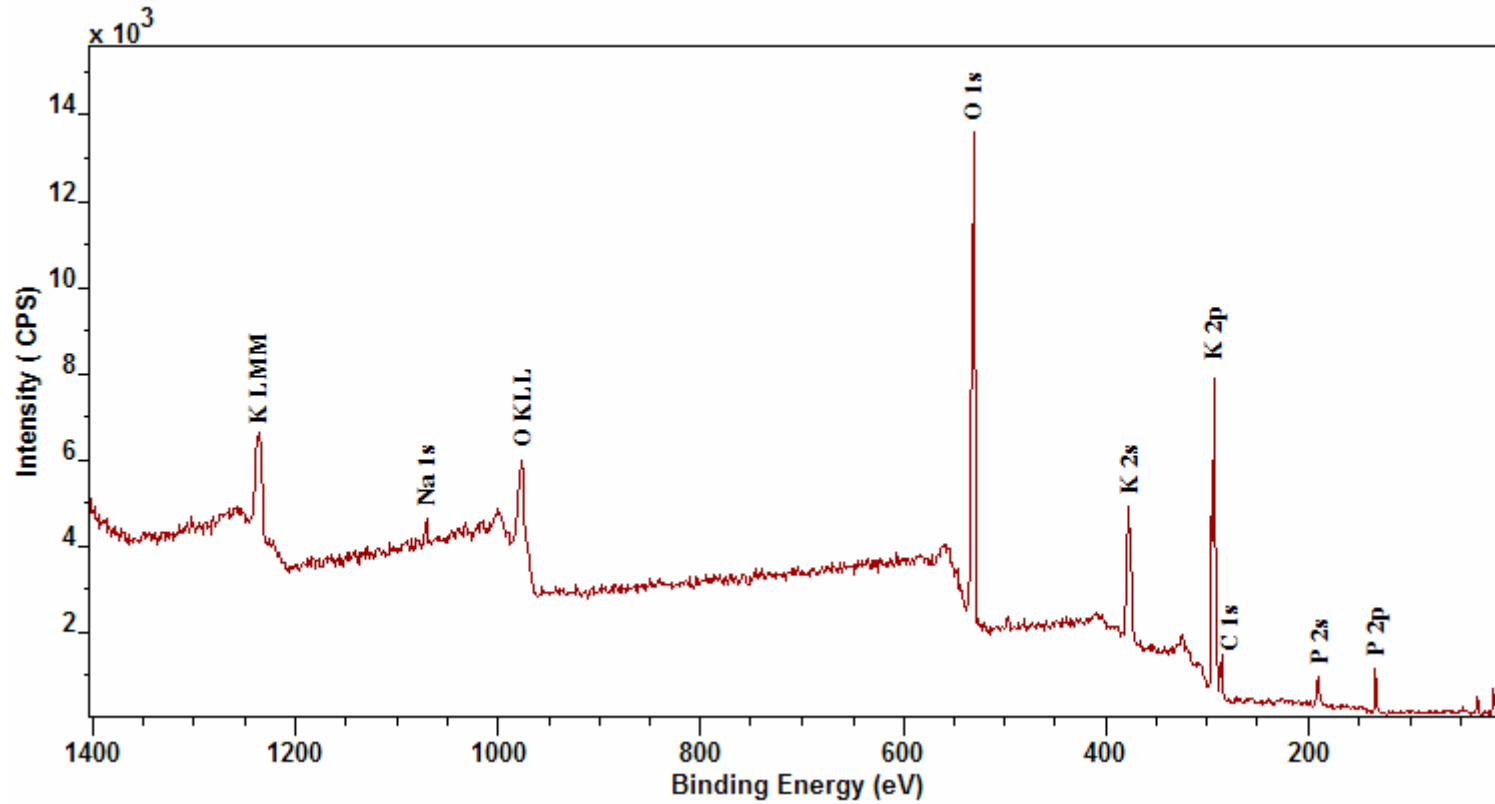
Printed using CasaXPS

KCl

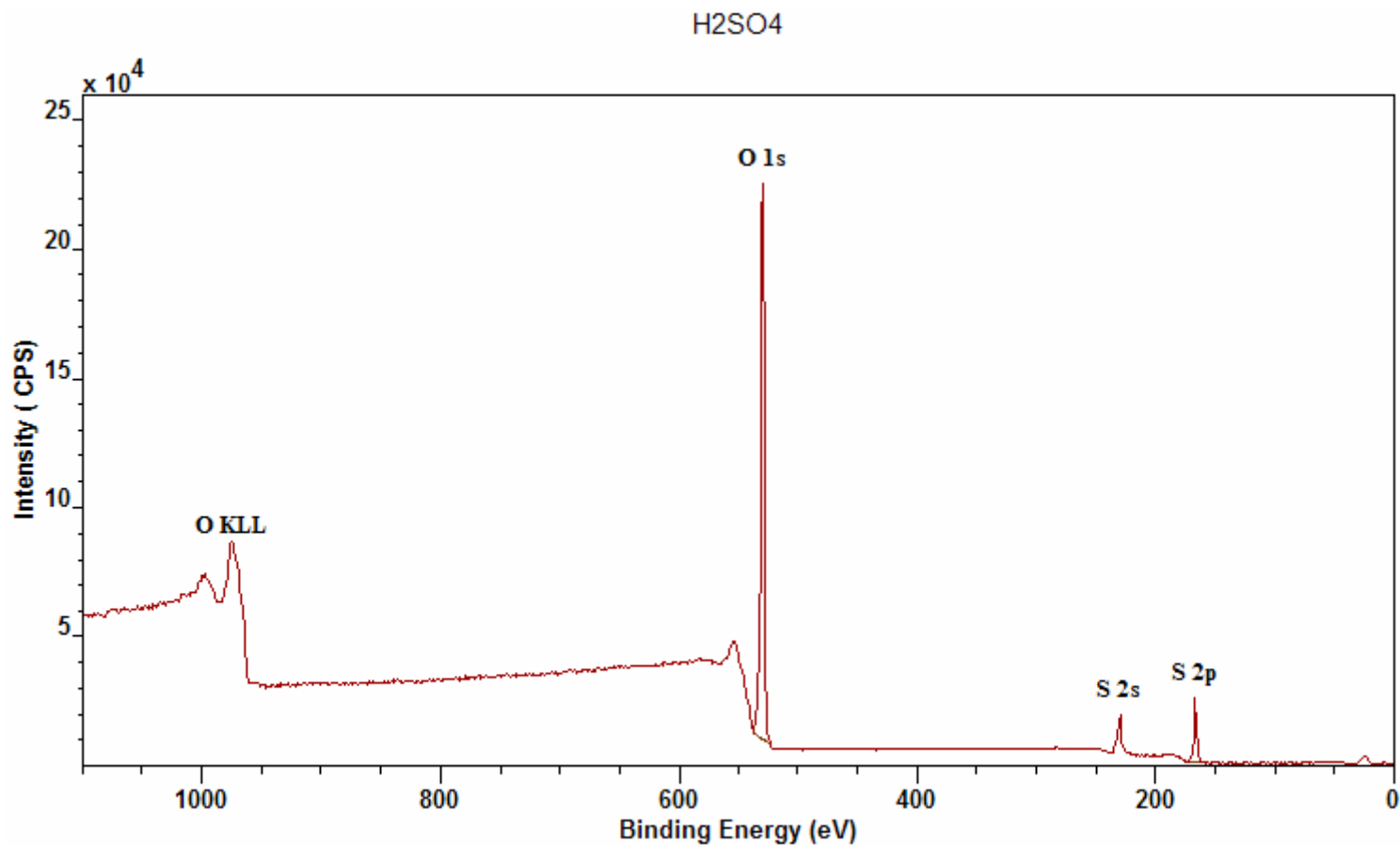


Printed using CasaXPS

K₂HPO₄



Printed using CasaXPS

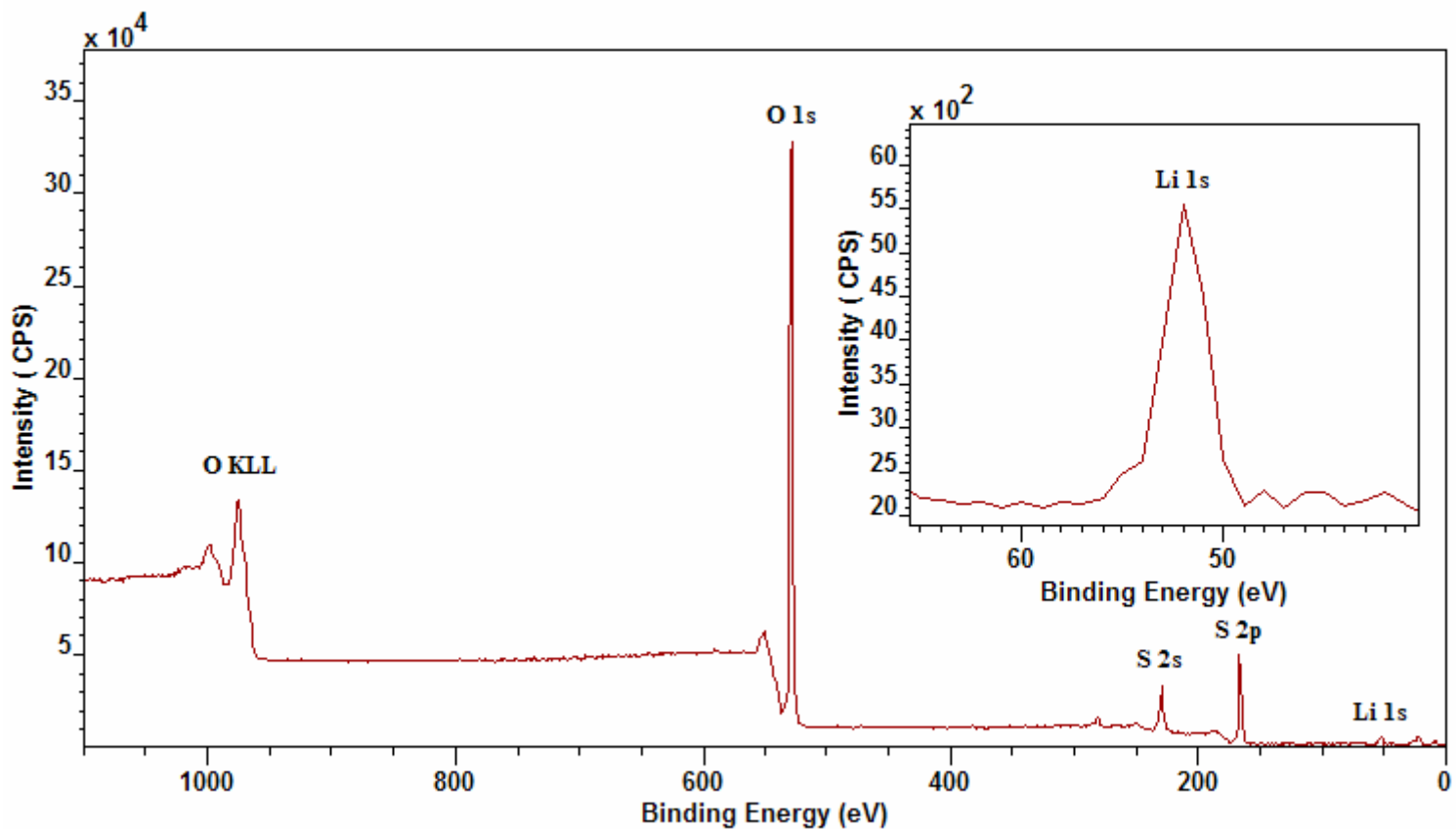


Printed using CasaXPS

XPS spectra and electronic structure of Group IA sulfates, M. Wahlqvist, A. Shchukarev / Journal of Electron Spectroscopy and Related Phenomena 156–158 (2007) 310–314

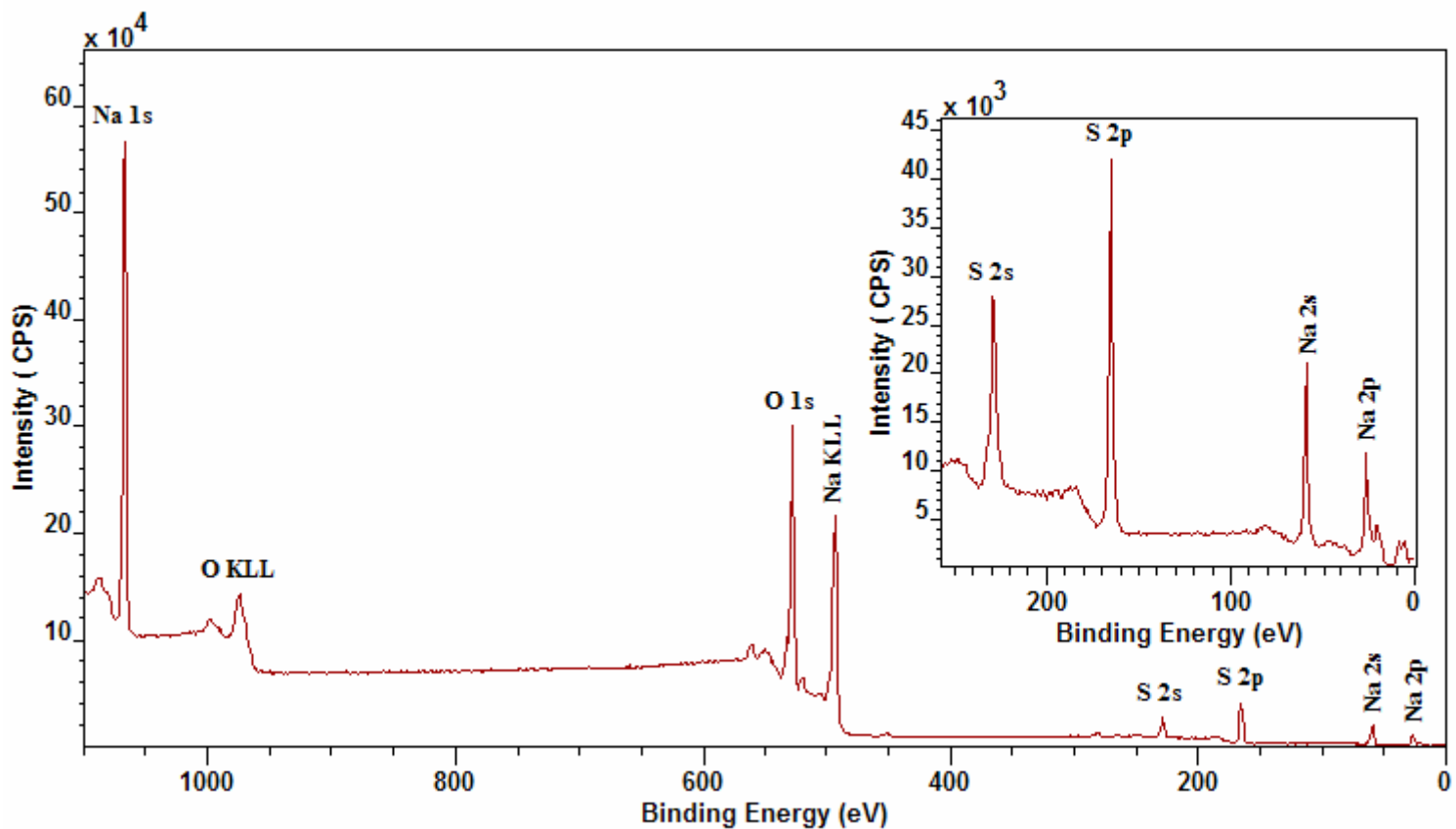
XPS Study of Group IA Carbonates, A.V. Shchukarev, D.V. Korolkov / CEJC 2(2) 2004 347-362

Li₂SO₄

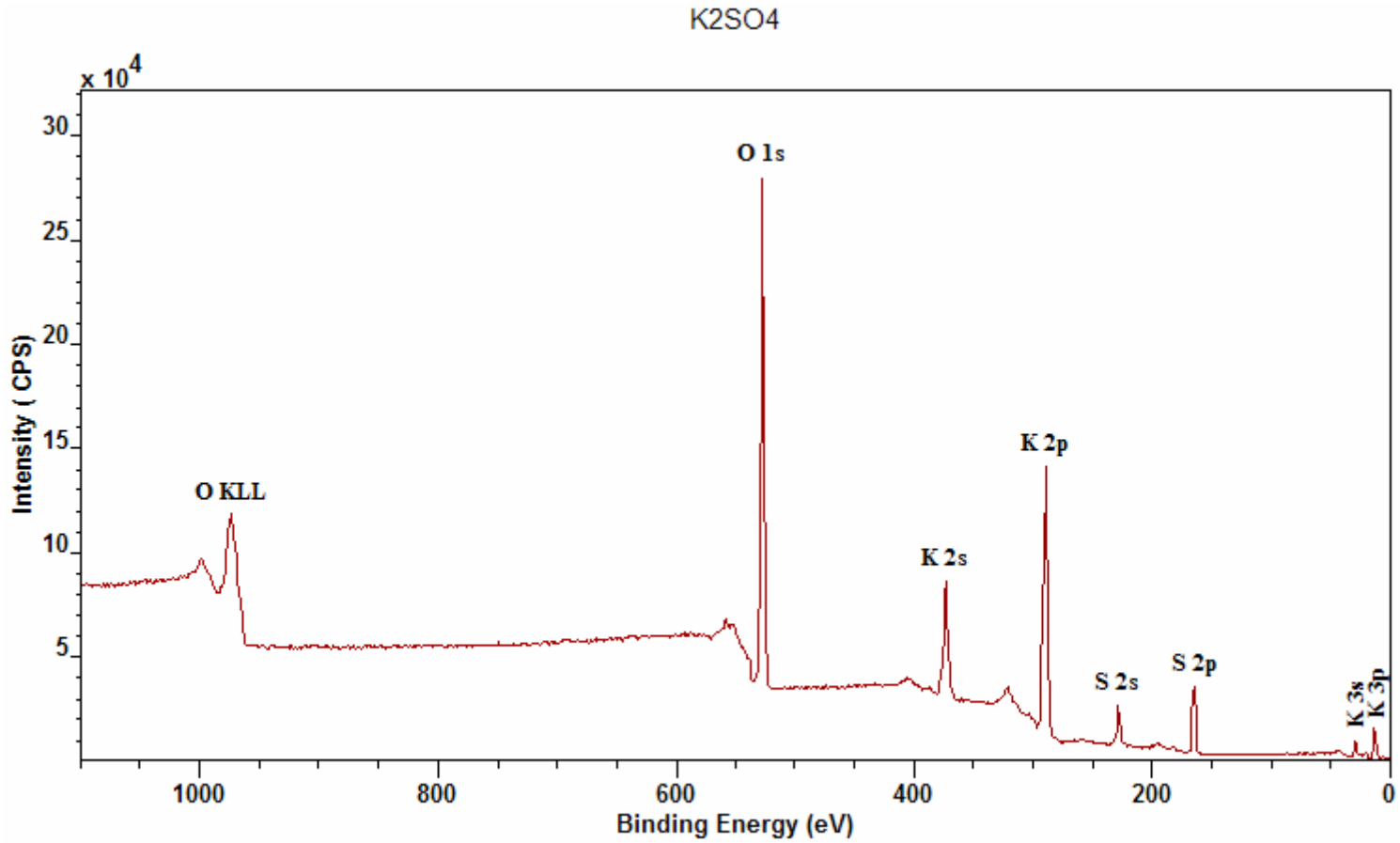


Printed using CasaXPS

Na₂SO₄

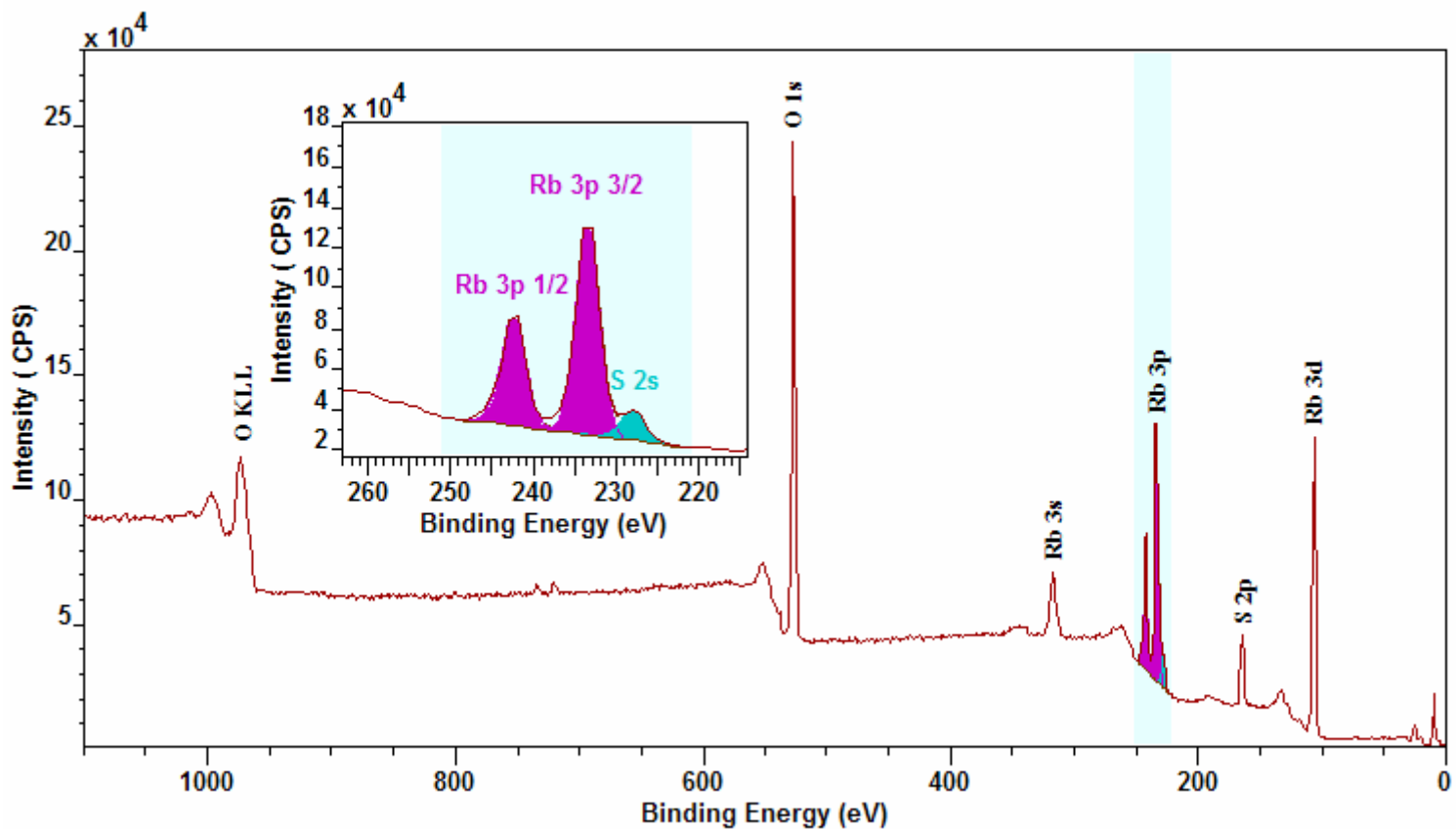


Printed using CasaXPS



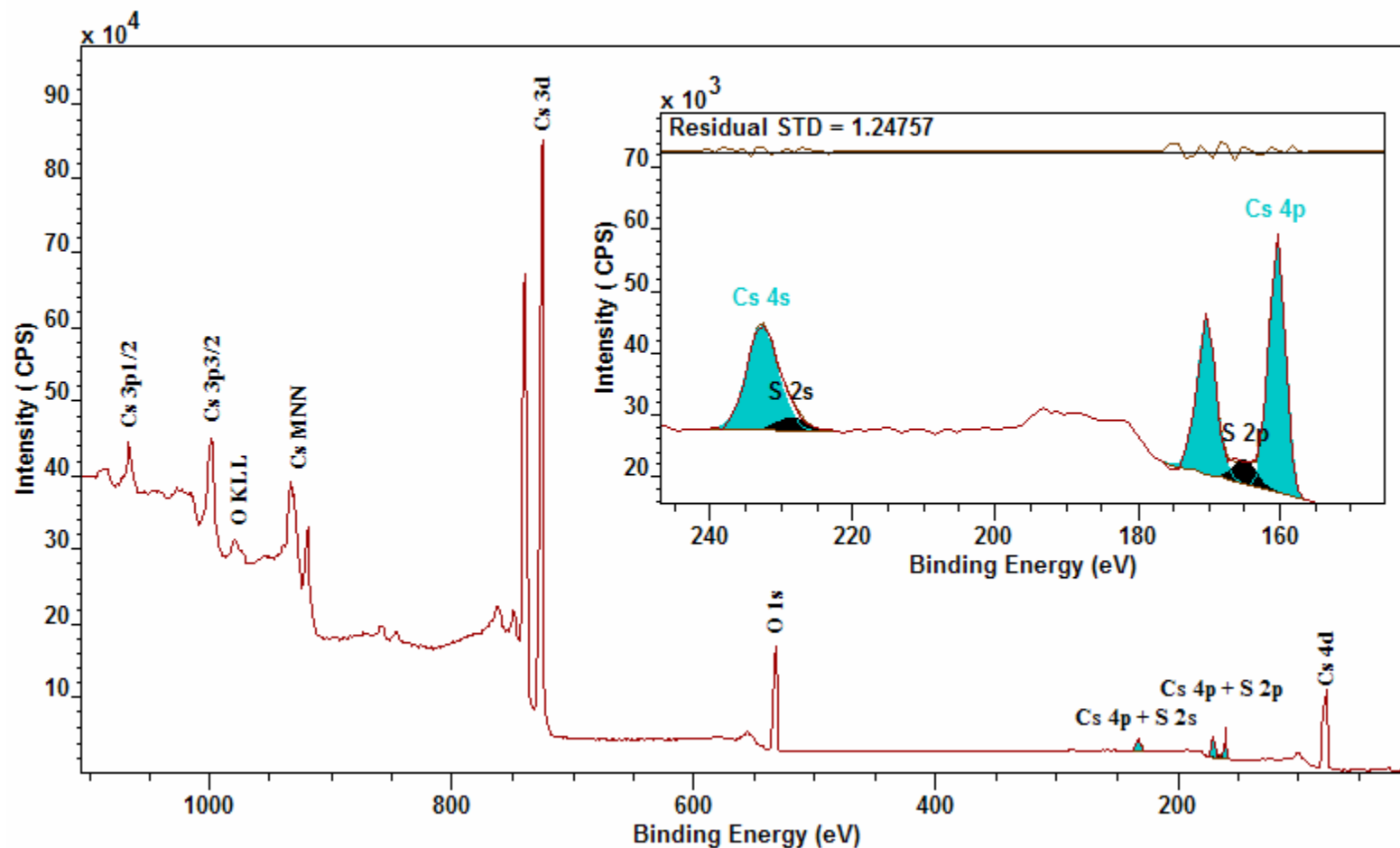
Printed using CasaXPS

Rb₂SO₄



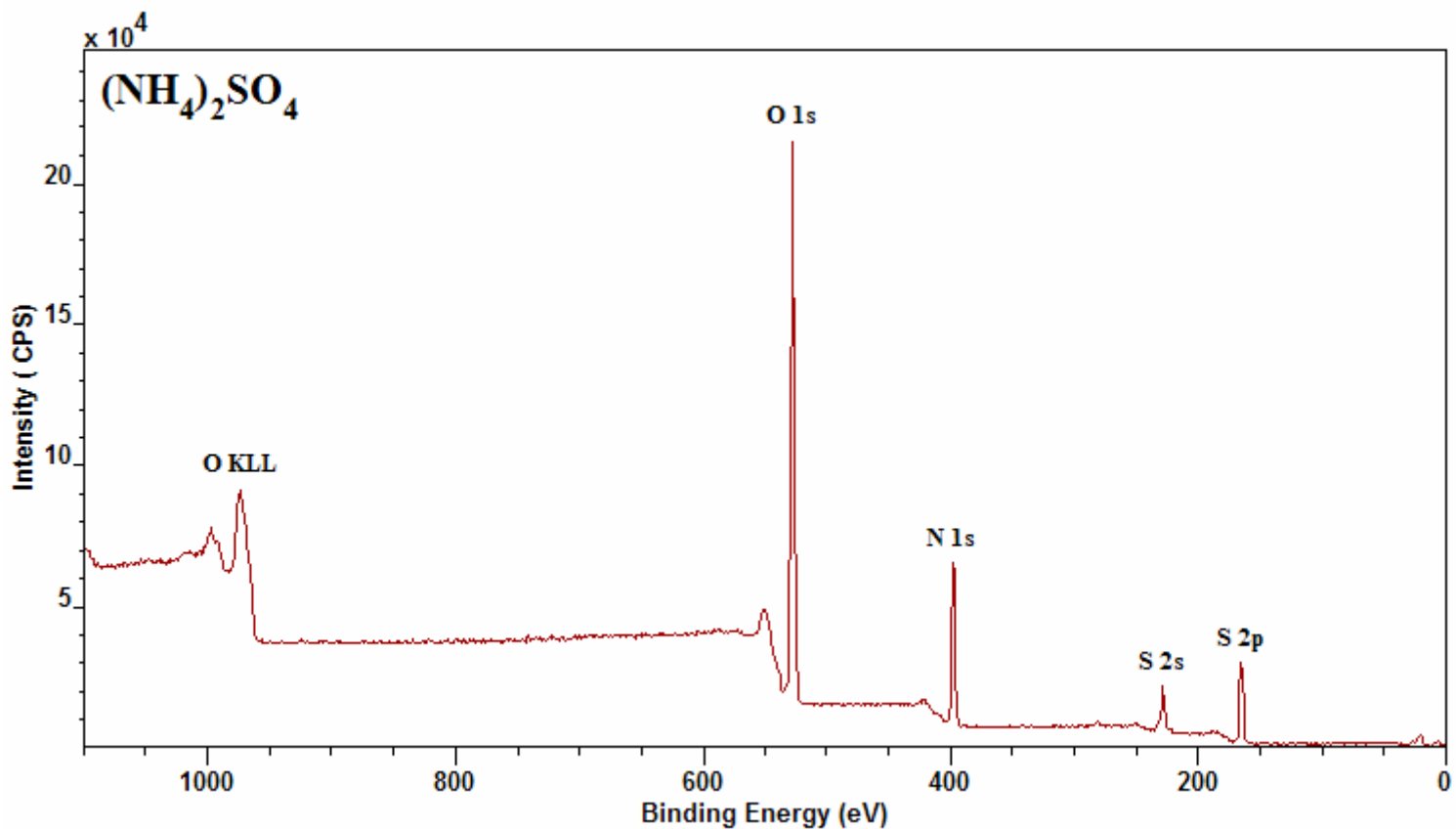
Printed using CasaXPS

Cs₂SO₄

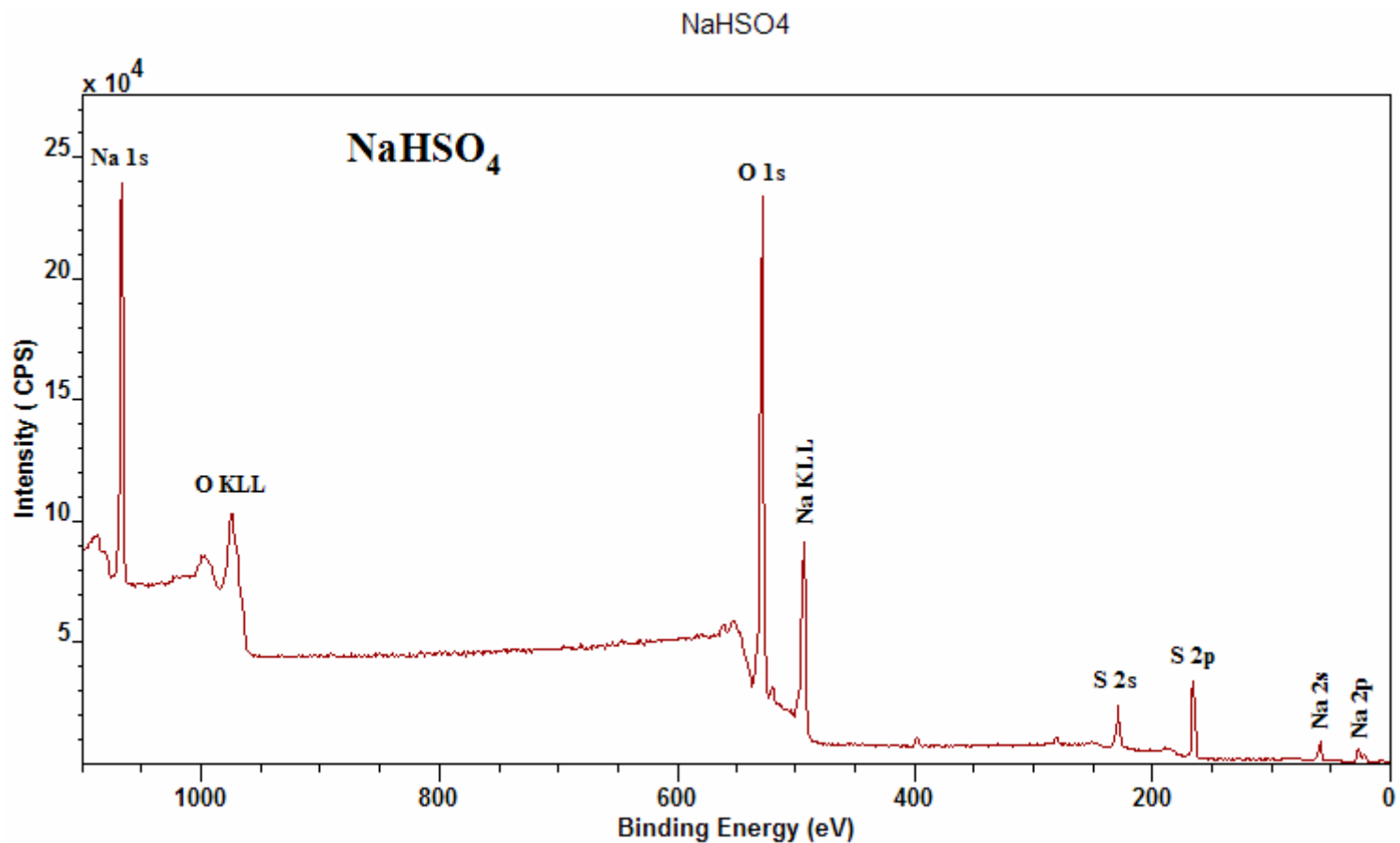


Printed using CasaXPS

Ammonium Sulphate

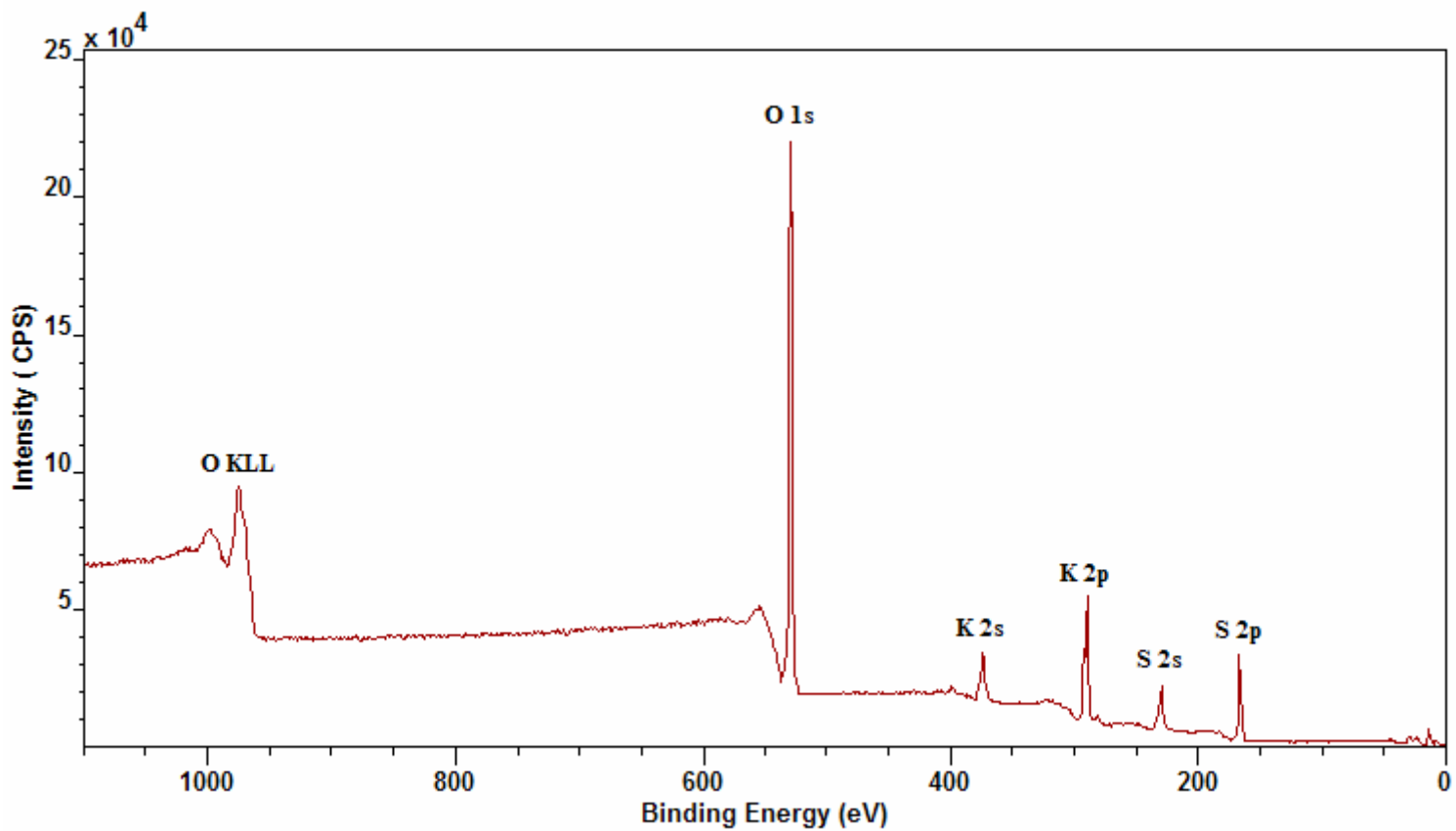


Printed using CasaXPS



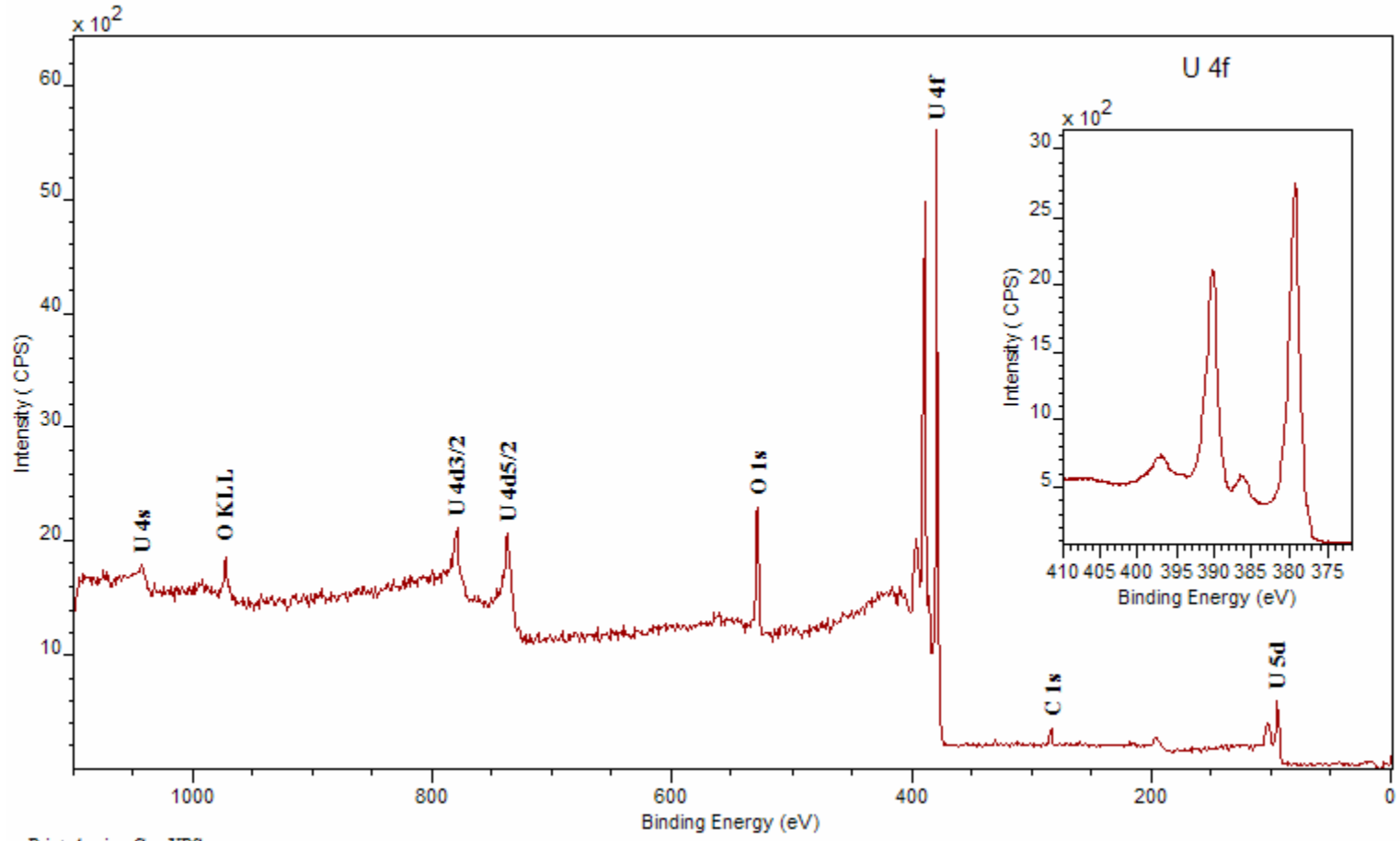
Printed using CasaXPS

KHSO4



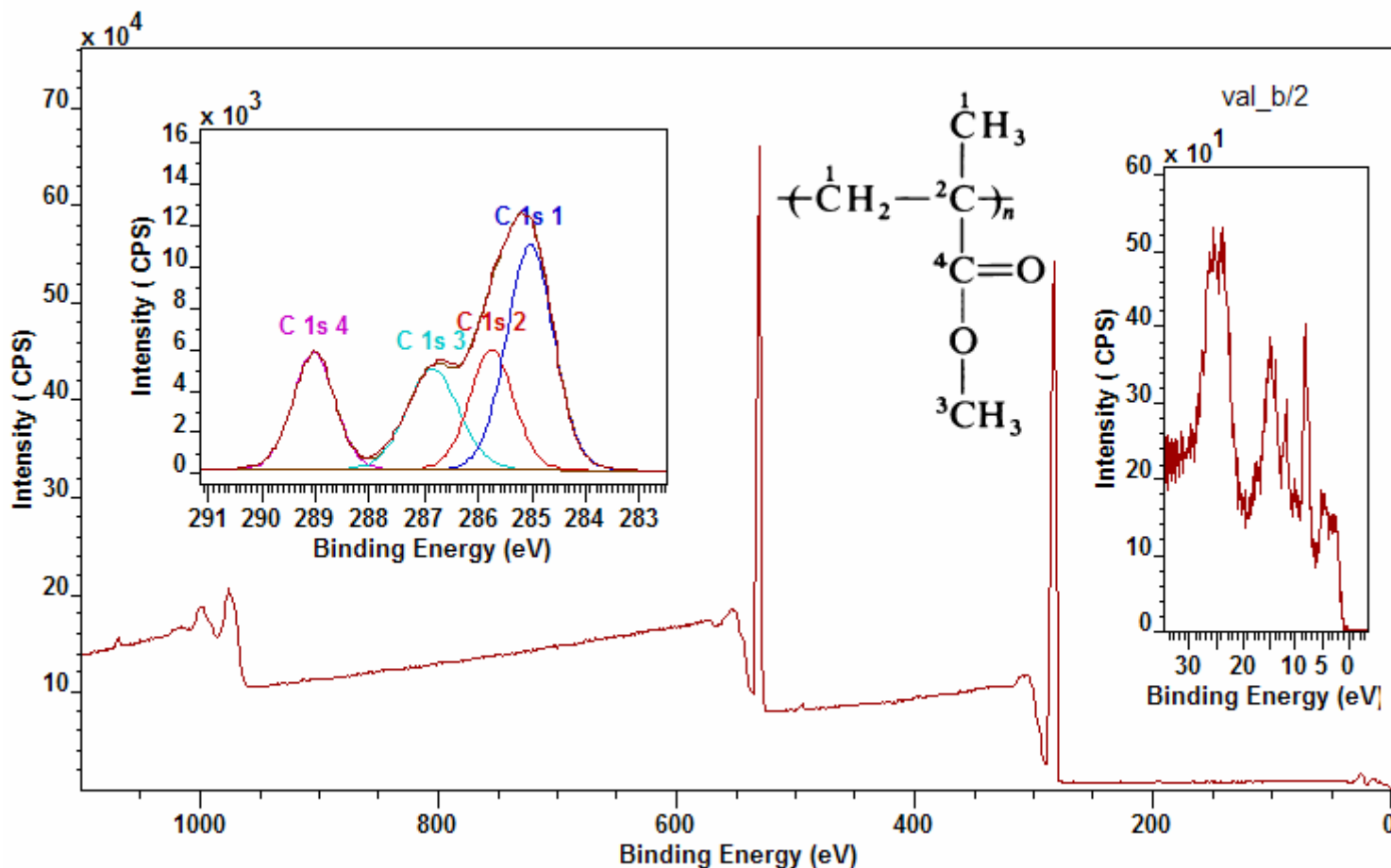
Printed using CasaXPS

UO₂



Printed using CasaXPS

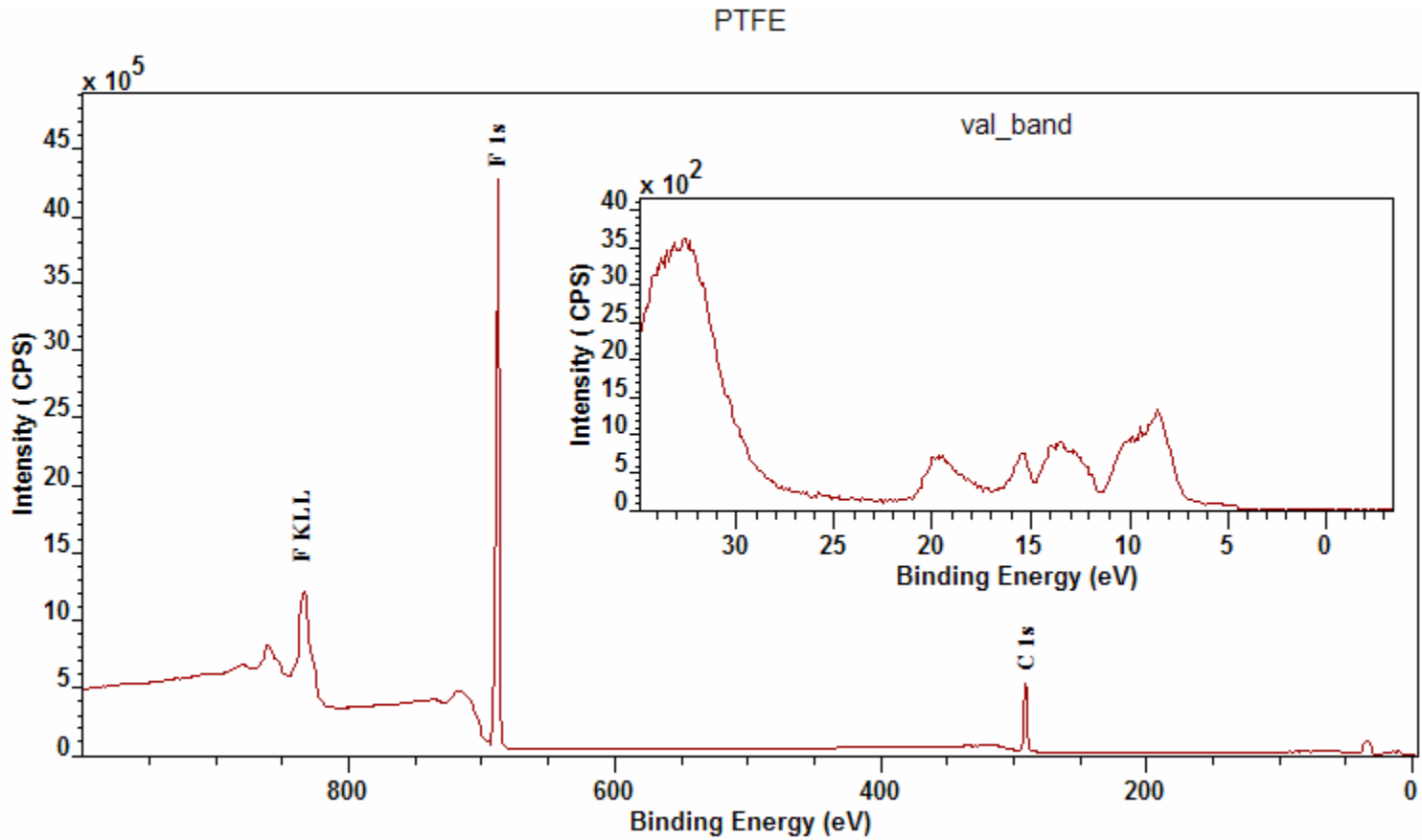
PMMA



Printed using CasaXPS

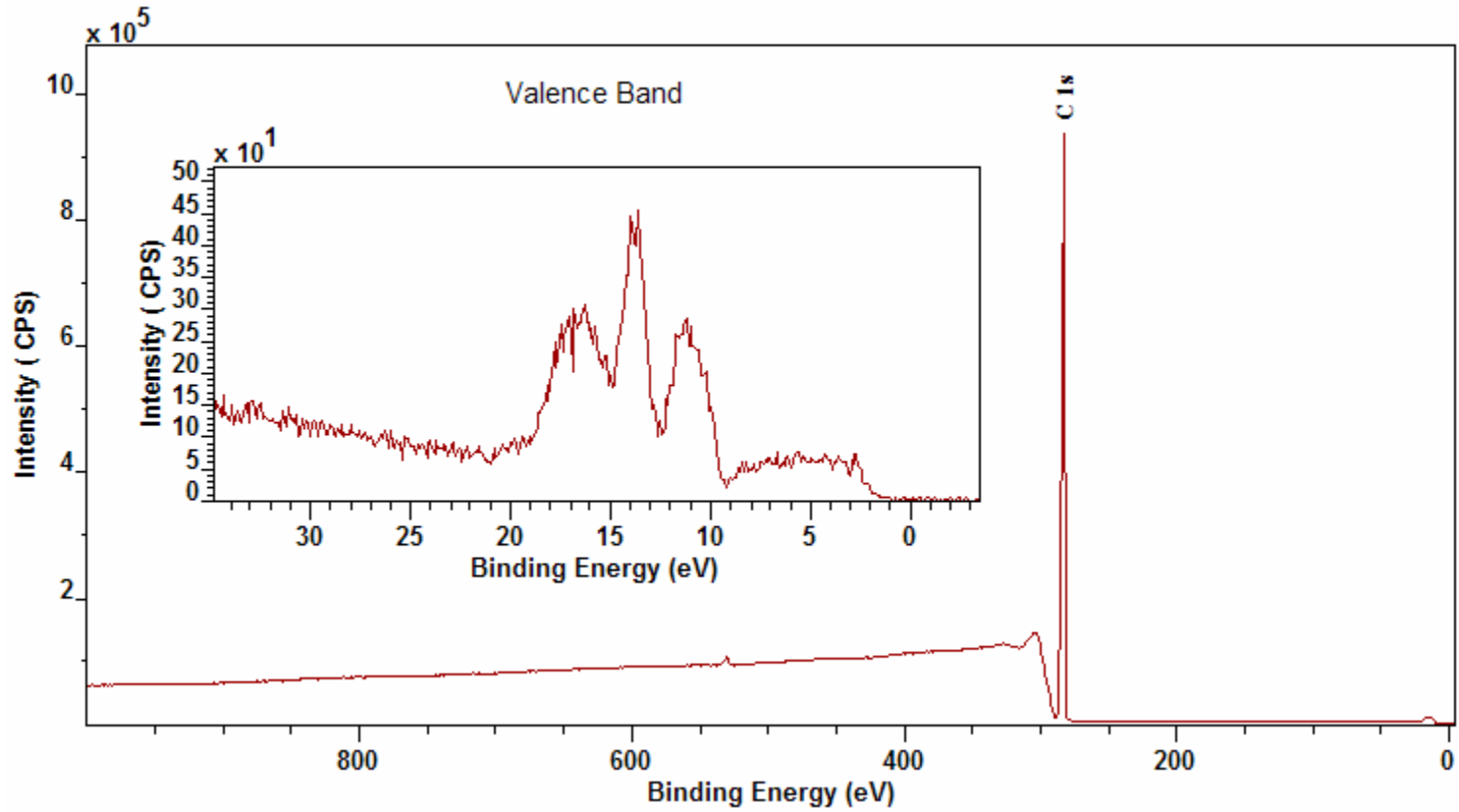
Poly(methyl methacrylate): C 1s peak assignments are based on those of Beamson and Briggs (The XPS of Polymers Database Edited by Graham Beamson and David Briggs (2000) ISBN: 0-9537848-4-3.

NCESS XPS Facility at Daresbury Laboratory, Warrington, UK <http://www.dl.ac.uk/NCESS/>



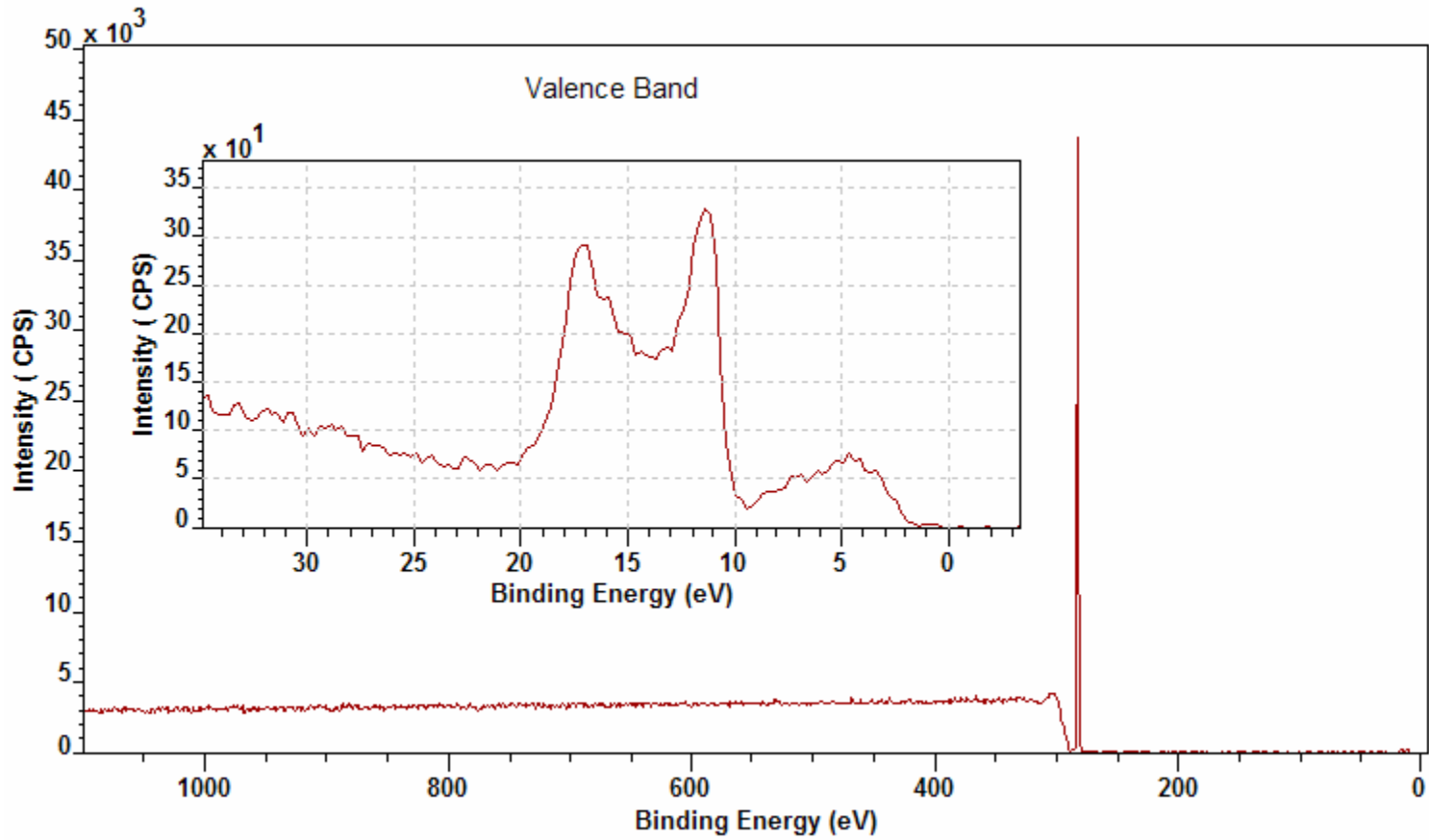
Printed using CasaXPS

Polypropylene



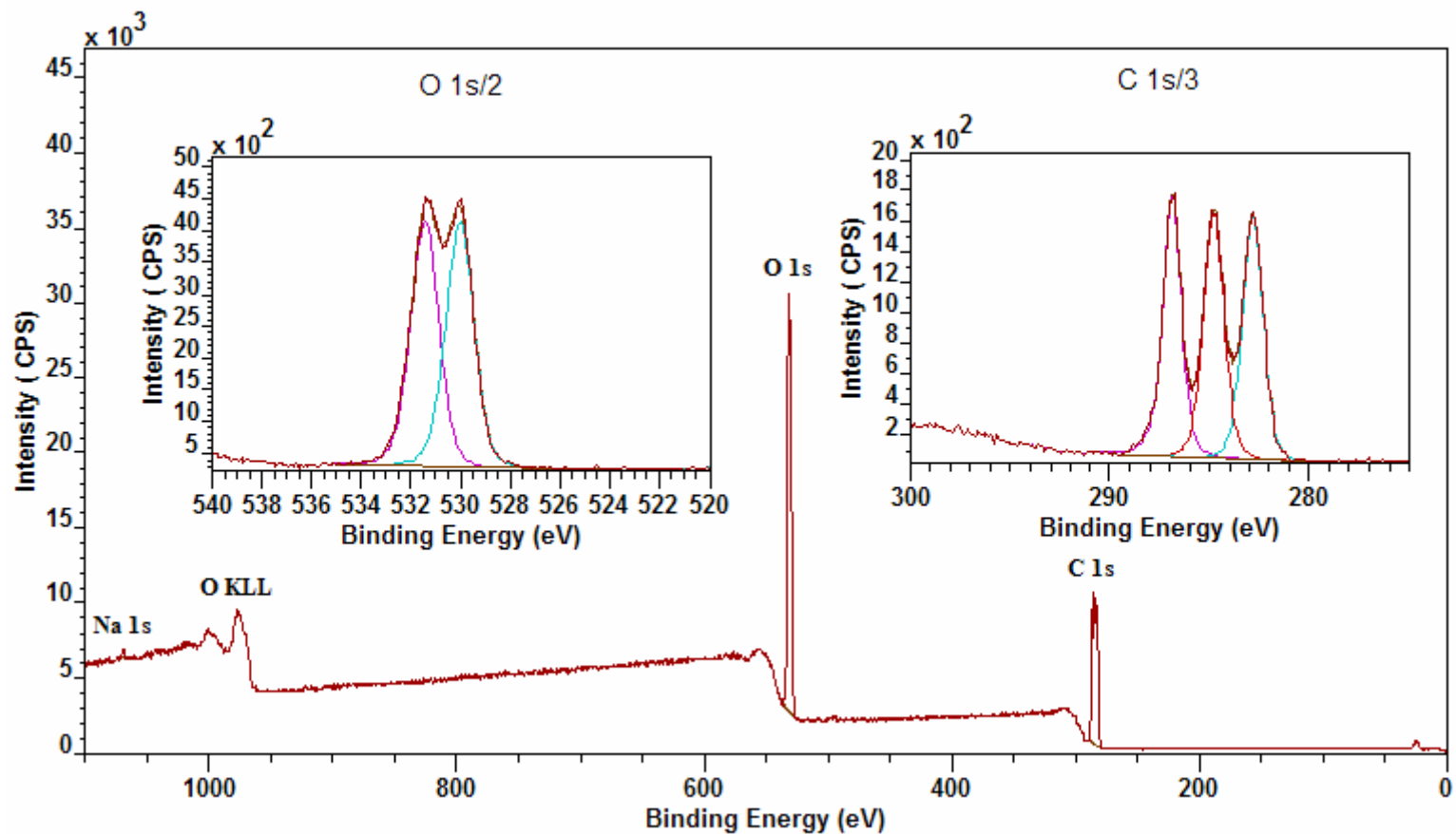
Printed using CasaXPS

Polyethylene



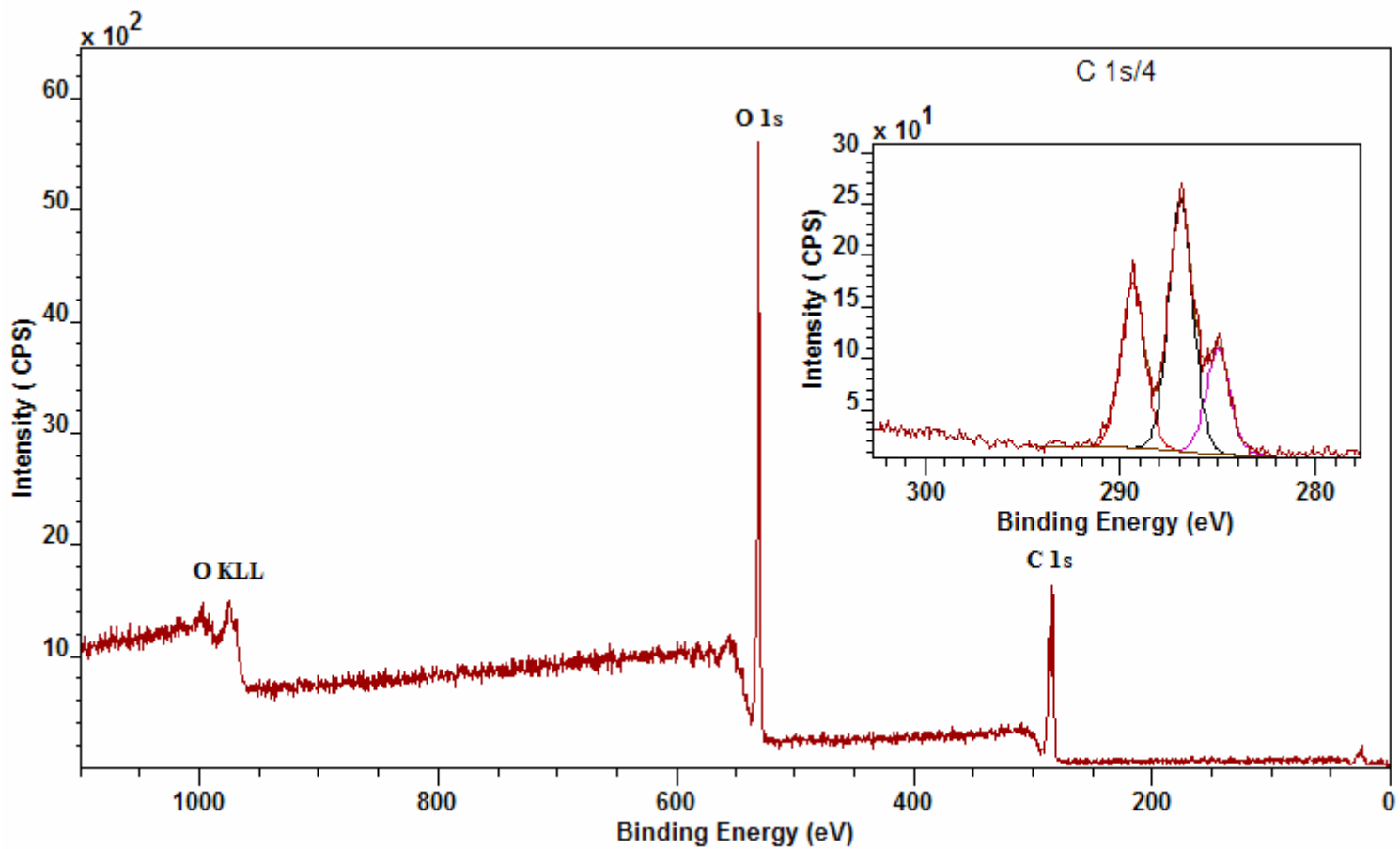
Printed using CasaXPS

Lacticacid



Printed using CasaXPS

Tartaricacid



Printed using CasaXPS



Copyright © 2008 Casa Software Ltd. www.casaxps.com

Acknowledgments

Data used to prepare this PDF were donated by:

University of Manchester, UK

University of Nottingham, UK

Peking University, China

Max Plank Institute Düsseldorf, Germany

Umeå University, Sweden

Lehigh University, USA

and several unnamed contributors.

A thank you to all involved in collecting these data.